FEATURE ARTICLE

ChemComm
www.rsc.org/chemcomm

Zeolite-based photocatalysts

Avelino Corma* and Hermenegildo Garcia*
Instituto de Tecnología Química, UPV-CSIC, Universidad Politécnica de Valencia, Av. de los Naranjos s/n, 46022 Valencia, Spain. E-mail: acorma@itq.upv.es; Fax: 34 96 3877809; Tel: 34 96 3877800

Received (in Cambridge, UK) 6th January 2004, Accepted 12th March 2004
First published as an Advance Article on the web 25th May 2004

The compartmentalised intracrystalline void space of zeolites are specially suited to incorporate and organise photoactive guests that can be used as photocatalysts. The rigid micropores allow assembly of multicomponent systems comprising of antenna and relays reminiscent of natural photosynthetic centers. Besides inorganic metal oxide clusters, zeolites as host are particularly attractive to construct organic photocatalysts since the guest becomes significantly stabilized by incorporation. This review gives special emphasis to the commercial and potential application of photocatalysts.

Zeolites are aluminosilicates whose crystal structure defines channels and cages of strictly regular dimensions. These empty intracrystalline spaces are in the nanometer or subnanometer length scale and are termed *micropores*. It is possible to accommodate a photoactive guest within the internal voids of these pores created by the rigid framework. The photoactive guests can be an organic photosensitiser, an inorganic semiconductor or a combination of both. In addition, the presence of heteroatoms (Ti, V and other transition metals) in the zeolite framework can make the structure as a whole act as a photocatalyst. This review is organized by grouping the photocatalysts according to the nature, organic or inorganic, of the guest or its location with respect to the zeolite framework.

The combination of a zeolite host and photoactive sites renders solid photocatalysts in which the high surface area and the adsorbent capacity provided by zeolites co-operate to increase the efficiency of the photocatalytic process. In addition, the zeolite pores define a compartmentalized space in which multi-component systems can be easily assembled by a stepwise procedure. Other positive effects derived from the encapsulation of a guest inside zeolites are a higher photostability of the sensitiser, the observation of quantum size effects for semiconductor clusters and a favourable polar environment for photoinduced electron transfer. Zeolite-based photocatalysts are promising for the abatement of air and water pollution using solar light, as well as for de-NOx and de-SOx processes, photoreduction of CO_2 by H_2O, photooxygenation of saturated hydrocarbons, photosplitting of water into hydrogen and oxygen, photogeneration of hydrogen peroxide and other photoprocesses of much current interest, particularly in environmental sciences and for the development of renewable energy resources alternative to fossil fuels.

Photocatalysis

There are two different ways in which the term photocatalysis can be validly used. In one of these, a photocatalytic process is when a single photon is able to form several molecules of products through a chain mechanism, performing several turnovers. One example of this definition is the electron-transfer chain mechanism of the cyclodimerization of 1,3-cyclohexadiene. By means of light a radical cation is formed that after reacting with neutral 1,3-cyclohexadiene forms a dimer radical cation which undergoes electron transfer to generate a [4+2]-cycloadduct and a new 1,3-cyclohexadiene radical cation. The driving force of the chain mechanism is that 1,3-cyclohexadiene radical cation is more stable than the [4+2]-cycloadduct radical cation. The latter starts a new cycle (Scheme 1).

In the above definition, a process is catalytic from the point of view of photons. A second use of the term photocatalysis is more common and derives from the similarity with thermal catalysis. It refers to a process in which a solid inactive as a thermal catalyst is able to absorb light and effect a transformation of substrates without appearing in the stoichiometry of the process or being consumed in the reaction. In this definition, the crucial element is a solid that transforms light into chemical energy, without being destroyed or consumed in the process.

Avelino Corma Canos was born in Moncófar, Spain. He was postdoctoral in the Department of Chemical Engineering at Queen's University (Canada, 1977–1979). He is director of the Instituto de Tecnología Química (UPV-CSIC) at the Universidad Politécnica de Valencia since 1990. His current research field is structured nanomaterials and molecular sieves as catalysts, covering aspects of synthesis, characterization and reactivity. Avelino Corma has written about 500 articles on these subjects in international journals, three books, and a number of reviews and book chapters. He is co-author of more than 80 patents, six of them being commercialised. He is the recipient of numerous awards including the Dupont Award on New Materials (1995), the Ciapetta and Houdry Awards from the ACS, the F. Gault Award of the European Catalysis Society and the Spain National Award on Science and Technology.

Hermenegildo García (Herme) was born in Canals (Spain) in June of 1957 and studied Chemistry at the Faculty of Science of the Universidad de Valencia (Spain) where he graduated in 1979 with Honors. He did his PhD on preparative organic photochemistry under the guidance of Professor Miguel A. Miranda and was awarded also with Honors by the Universidad de Valencia in 1983. Then, he moved to the Technical University of Valencia where he initiated his career in 1983 first as Assistant Professor, becoming finally Full Professor in 1996. In 1991 he was appointed member of the Institute of Chemical Technology, a joint centre depending on the Spanish National Research Council (CSIC) and the Technical University of Valencia that was founded in that year. He did a postdoctoral stay at the Chemistry Department of the University of Reading (UK) with Professor Andrew Gilbert in 1987, and later three successive sabbatical leaves in 1992–1993 (one year), 1995 (six months) and 2000 (three months) at the University of Ottawa joining the Laser Flash Photolysis group headed by Professor J.C. (Tito) Scaiano. He has co-authored over 200 papers most of them dealing with the application of zeolites as hosts of organic guests and as solid catalysts. He held three international patents. His main current interests are in supramolecular photochemistry and photocatalysis, development of photoactive nanoscopic materials and heterogeneous catalysis.

DOI: 10.1039/b400147h

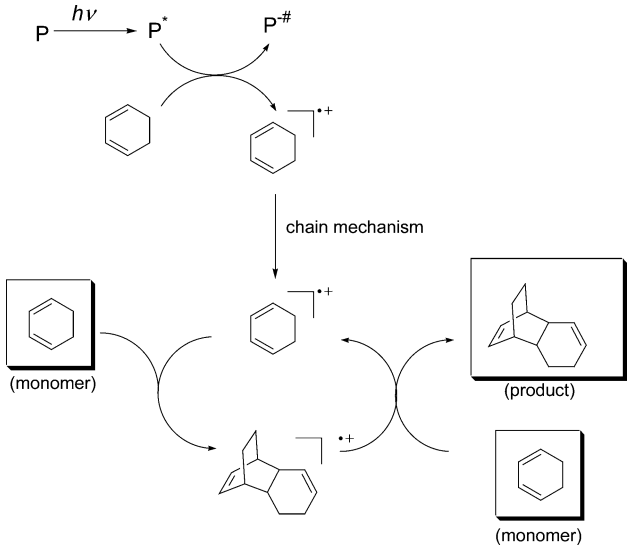

Scheme 1

Semiconductors are typical inorganic photocatalysts. In this case, light absorption excites one electron from the valence to the conduction band (Scheme 2). The mobility of the excited electron

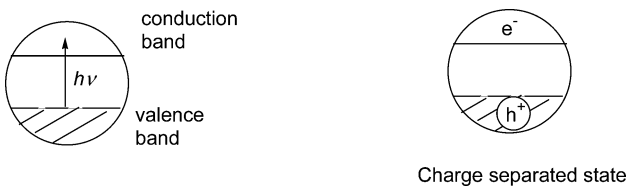

Scheme 2

in the conduction band may lead to charge separation with the creation of positive vacancies in the valence band (*holes*, h^+) and mobile electrons (e^-) in the conduction band. This charge separation combined with interfacial electron transfer processes from the surface of the semiconductor particle to the substrate is the base of photocatalytic processes. The efficiency of the photocatalyst is a function of the balance between charge separation, ease of interfacial electron transfer and energy-wasting charge recombination.

Organic photocatalysts are less common due to their poor photostability and the ease in which they undergo self-decomposition. In this case, the organic photosensitiser reaches a singlet electronic excited state that after intersystem crossing may reach the triplet manifold (Scheme 3). Singlets are shorter-lived (typically ns) and triplets are much longer-lived (μs time scale). Excited states are always considerably stronger electron donors (the excited electron occupying a high energy orbital) or electron acceptors (accepted in the semi occupied low-energy orbital) than the closed-shell ground state and thus they can easily participate in electron transfer processes. Charge separation may occur, as in semiconductors, if the organic molecule reacts with an electron donor or acceptor substrate.

This review covers the literature up to 2002 and focuses on those reports that describe the use of zeolites as a solid matrix or rigid host to incorporate or embed a photoactive host, the resulting supramolecular assembly being able to act as a photocatalyst. Among the advantages of zeolites as hosts, the one that makes these solids very attractive as hosts is their large surface area and internal pore volume. Surface areas in the range 400–650 $m^2\ g^{-1}$ with pore volumes of above 0.1 $cm^3\ g^{-1}$ are not uncommon for conventional zeolites. In fact, zeolites are among the most porous materials known, being suitable to adsorb guests.[1,2] A brief summary of the main structural characteristics of the zeolites is pertinent.

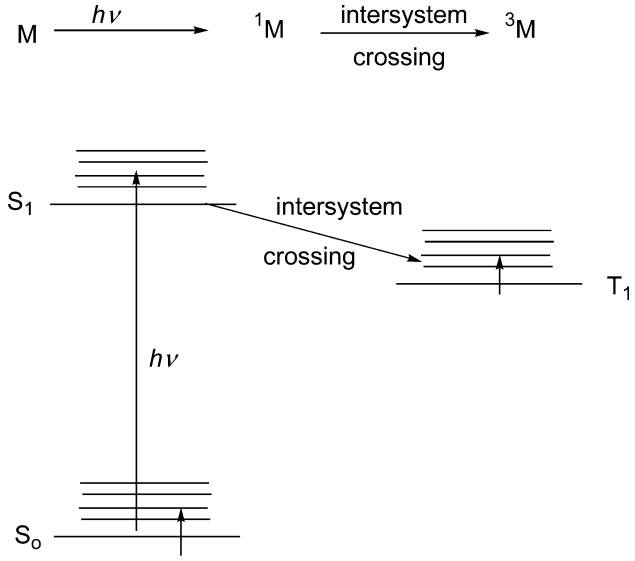

Scheme 3

Zeolites and molecular sieves acting as hosts for photoactive guests

Zeolites are crystalline aluminosilicates whose rigid structure define channels and cavities of strictly regular dimensions called micropores.[1–3] These micropores in the nm range are open to the exterior of the particle, thus allowing mass transfer from the surrounding solution to the interior of the particle. The ability of zeolites to incorporate and adsorb an organic guest gives rise to a *supramolecular* chemistry where the intrinsic *molecular* properties of the adsorbate can be modified and even controlled by its interaction with the rigid walls of the zeolite or by the presence of active sites in the pores.

The geometry of the internal voids and the dimensions of the pores vary depending on the crystal structure of the zeolite.[4] In this regard, the zeolites can be classified as small, medium, large and extra-large pore zeolites depending on whether the number of framework O and T atoms (T=Si, Al or any other framework heteroatom) that defines the pores are 8, 10, 12 or more.[5,6] According to the topology of the pore system, the zeolites can also be classified as mono-, bi- and tridirectional depending on whether the pores are arranged along one, two or the three Cartesian axes (Scheme 4).

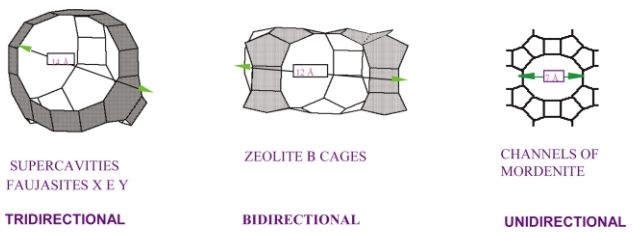

Scheme 4

Tridirectional, large-pore zeolites such as faujasites X and Y (supercages arranged tetrahedrally) and bidimensional zeolite Beta are the most widely used for the purpose of guest inclusion. The reason for this is the presence of large cavities with dimensions around 1.1–1.4 nm that are interconnected and arranged tridirectionally. These values are among the largest pore dimensions that are available for conventional zeolites.

The empty voids of the dehydrated zeolites provide a compartmentalized space in which photosensitisers can be located or where multi-component systems can be assembled in a spatially organized manner and held in place without the need of covalent bonds.[7] This situation is somehow reminiscent of the photosynthetic centres of green bacteria, algae and plants in which the

different components are organized and structured spatially in order to harvest light efficiently. The term *mechanical immobilization* has been coined by Stoddart to describe those supramolecular systems in which the components are held without existing covalent bonds between them.[8–10] This is the case of [2]-catenanes in which two macrocyles are interlocked and interpenetrated, but they are not connected by inter-ring covalent bonds[11] and this is also the case where a large guest is entrapped inside a zeolite cage being too big to escape through smaller cavity windows.

Zeolites and related molecular sieves exhibit several specific features that make them suitable for their use as hosts for photosensitisers, such as:

(i) full photochemical stability and large thermal and chemical inertness,

(ii) transparency to UV-Vis radiations above 240 nm thus allowing a certain penetration of the exciting light into the solid opaque powder to reach the guests located in intraparticle positions,

(iii) the possibility to vary the chemical composition of framework and out-of-framework positions in a large extent, thus rendering these molecular sieves photoactive or introducing active sites to co-operate in the photocatalytic activity,

(iv) zeolite high adsorptivity for organic compounds in solution, aiding to the concentration of the substrates in the proximity of the photosensitiser contributing to the success of the photocatalytic process,[12]

(v) modulation of the micropolarity and the polarizing strength of the zeolite interior by varying the nature of internal charge-balancing cations (charge density) and the size of the channels. The latter factor can lead to dramatic changes and modifications in the electronic states and conformational mobility of the guests within zeolites,[13–15] and

(vi) ability of the zeolite framework to participate actively in electron transfer processes, either as electron acceptor or electron donor.[17] Thus, upon photoexcitation, an incorporated guest can eject an electron that will become delocalised through the framework or in clusters of the charge balancing cations. Also, the reverse process in which electron-rich sites of the zeolite can donate an electron to photoexcited guests are known.

On the negative side of the use of zeolites as matrix there are some disadvantages related to zeolite encapsulation of photosensitisers such as:

(i) a *dilution effect* in the sense that for a given weight of solid, the active component is only a certain percentage of the total, and

(ii) the fact that the preparation of the encapsulated photocatalyst requires extra steps of manipulation and processing and the difficulty to check for purity and distribution of the incorporated guests.

Irradiation procedures and photocatalytic reactors

An additional disadvantage inherent to all photochemical reactions using solids are optical phenomena associated with the use of opaque powders. These phenomena are related to the interaction of the light with the solid such as light scattering, diffraction and reflection. A key issue that has to be properly addressed is the problem of photoreactor design in order to accomplish the optimum exposure of the maximum solid surface to the radiation. These drawbacks are, however, common for any powdery solid photocatalyst. For this reason, irradiation of dry powders is frequently inefficient as compared to transparent solutions and requires long exposure times or gives rise to low conversions.[12] Considering the energy costs, this is a major drawback that has not yet been fully satisfactorily solved, particularly at large volume scales. Compared to irradation of dry powders, a much more efficient irradiation procedure consists of the illumination of a solid–liquid suspension or slurry of the solid photocatalysts that can be continuously stirred. In this case, the liquid may contain the substrates and products, but these systems have to be surveyed in order to assess the heterogeneity of the process and specifically for the fact that the liquid phase does not contain any dissolved photocatalytically active species leached from the solid to the solution.

While photocatalytic irradiations of suspensions are common practice at laboratory scale, it can only be applied to batch-like processes, while immobilization of the photocatalyst in a *fixed bed* would be preferred for continuous flow reactions.[12] The design of efficient photoreactors for liquid phase photoreactions, the geometry of the light source and disposition of the solid in films are issues of paramount importance in order to optimise energy costs. In this regard, it has been reported that optical microfibers can be coated with zeolite crystals. The process consists in grafting covalently zeolite crystals onto the optical fibers using tetraethyl orthosilicate *via* a sol–gel process.[16] As a reflection of the more efficient excitation of the zeolite particles, the coated optical fibers exhibit superior photocatalytic activity for the photooxidation of trichloroethylene and dichloromethane. This photocatalytic device can stand thermal regeneration, in which a 78% of the initial activity of the fresh system can be restored. This type of approach to provide light in an efficient way close to the photocatalytic centre can be useful in the future development of more efficient photocatalytic devices.

It is clear that more efforts are still necessary for the design of commercial photocatalytic reactors, this requiring a study of the hydrodynamics of the reactor coupled with the intrinsic rate kinetics of the photocatalytic process. Reported annular fluidised-bed photocatalytic reactors allowing *in situ* regeneration of the photocatalyst are also very attractive as photoreactors for large scale processes.[12]

Zeolites containing a photoactive organic dye

Electron donor photosensitisers

Ruthenium(III) trisbipyridyl has been one of the favourite photoactive complexes to study photoinduced electron-transfer processes inside the zeolite micropores.[17] $Ru(bpy)_3^{2+}$ in its excited state is a good electron donor and in the presence of electron acceptors undergoes a transformation to $Ru(bpy)_3^{3+}$. $Ru(bpy)_3^{3+}$ is a relatively stable complex that can even be prepared as an indefinitely stable species by dissolving $Ru(bpy)_3^{2+}$ in strongly acidic media. The major advantages of $Ru(bpy)_3^{2+}$ as photosensitiser are the long wavelength absorption ($\lambda_{max} \sim 460$ nm) that allows selective excitation of the complex in the presence of quenchers and the relatively intense, long-lived emission ($\lambda_{em} \sim 600$ nm, τ in the μs time domain) that allows the use of conventional time-resolved fluorimeters to monitor the evolution and behaviour of the system.

$Ru(bpy)_3^{2+}$ can be synthesized inside the zeolite Y cavities by ship-in-a-bottle synthesis, a term that was originally coined by Herron[18,19] to describe the preparation of related large metallic complexes (such as metal salen[19] and metalloporphyrins[20] and metallophthalocyanines[21]) inside the cavities of zeolites through the formation of coordination bonds between the ligand and the metal ion resident inside the zeolite micropores. There have been published in the literature excellent reviews giving proper credit to the pioneers of this chemistry.[22–27] The actual preparation procedure for $Ru(bpy)_3^{2+}$ encapsulated within zeolites derives from the synthetic method described by Lundsford,[28] later improved by Dutta consisting in the reaction of an excess of 2,2-bipyridine at 200 °C with $Ru(NH_3)_4^{3+}$ previously exchanged in NaY zeolite (Scheme 5).[29–31] The origin of the electron gained spontaneously in

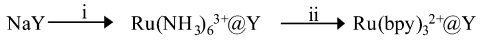

i) $Ru(NH_3)_6^{3+}$

ii) excess of 2,2'-bypyridine (bpy) / 200 °C, 24 h / exhaustive extraction solid-liquid

Scheme 5

the process of ligand exchange from $Ru((NH)_3^{3+}$ to $Ru(bpy)_3^{2+}$ is yet to be revealed.

A considerable amount of work has been carried out with the $Ru(bpy)_3^{2+}$-bipyridinium (either 2,2′- or 4,4′-) as donor–acceptor couple adsorbed or supported on zeolites.[17]

Viologens are compounds having a chemical structure of 4,4′-bipyridinium dication and they are easily introduced in zeolites by ion exchange. The positive charge of the aromatic rings together with the presence of electronegative N atoms makes bipyridiniums strongly electron acceptor compounds. In addition, viologens normally do not emit,[32] they have an absorption at ~280 nm and have radical cations easily characterizable by UV/Vis spectroscopy, the combination of all these features making these compounds an ideal couple for electron transfer with $Ru(bpy)_3^{2+}$. Quenching of $Ru(bpy)_3^{2+}$ triplet excited state by viologen can be monitored by fluorescence or optical absorption spectroscopy (either time-resolved in the submillisecond time domain or conventional when the viologen radical cation is sufficiently stable), thus allowing the study of the kinetics and quantum yields of the interaction between $Ru(bpy)_3^{2+}$ and viologens.

Considering the zeolite as a host defining a constrained space, most of the possible situations for the $Ru(bpy)_3^{2+}$–viologen pair have been already reported, for instance, (i) $Ru(bpy)_3^{2+}$ outside the pores and viologens inside the pores, (ii) $Ru(bpy)_3^{2+}$ inside the cages and size-excluded viologens outside, (iii) both $Ru(bpy)_3^{2+}$ and viologens inside the same particle, (iv) $Ru(bpy)_3^{2+}$ in one particle and viologen in another zeolite particle, (v) viologen and $Ru(bpy)_3^{2+}$ in separate cavities of the same particle,[33] (vi) $Ru(bpy)_3^{2+}$ and viologen derivatives covalently bound and supported on zeolites, *etc.* For an in-depth coverage the $Ru(bpy)_3^{2+}$-zeolite systems, the reader should refer to previous reviews on the topic,[17] including an excellent introduction by Yoon and co-workers.[34]

One interesting recent contribution using the $Ru(bpy)_3^{2+}$–viologen/zeolite system provides convincing evidence that light excitation can be used to pump electrons from the zeolite framework to an electron acceptor (viologen) located outside the zeolite.[34] This has been demonstrated by irradiating with visible light a suspension of K^+-exchanged Y zeolite containing $Ru(bpy)_3^{2+}$ encapsulated inside the zeolite supercages in acetonitrile containing the bulky dicyclohexyl derived viologen that is size-excluded from the pores of KY zeolite.

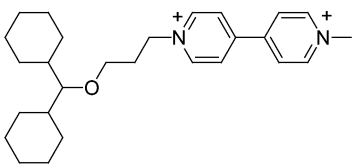

N-(3-dicyclohexylmethoxy)propyl-N'-methyl-4,4'-bipyridinium

The electron transfer from internal excited $Ru(bpy)_3^{2+}$ towards external viologen is mediated by K^+ migration to accomplish the electroneutrality of the system. Addition of crown ethers able to complex K^+ retards sufficiently the back electron transfer to allow the quantitative determination of the viologen radical cation by using a conventional spectrophotometer and applying the Lambert–Beer law and the solution extinction coefficients. Moreover, the yield of viologen radical cation increases up to a factor of 10 when the acetonitrile solution contains a suitable crown ether to bind K^+. Quantification has established that the amount of viologen radical cation is about 50 times higher than that of $Ru(bpy)_3^{2+}$ present in the system.[34] This fact has been interpreted as demonstrating a photoinduced *vectorial* (following a single sense) electron pumping from the zeolite framework to the viologen, the photoactivable redox $Ru(bpy)_3^{2+}/Ru(bpy)_3^{3+}$ couple acting as the pump fuelled by light (Scheme 6). Some thermal pumping was also observed

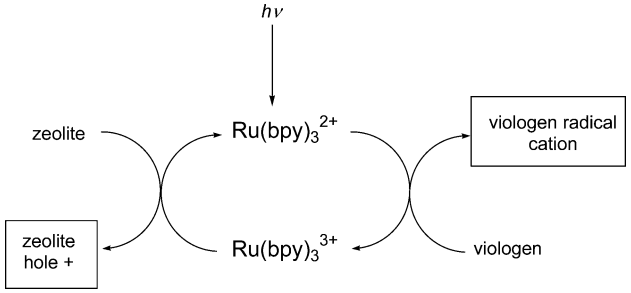

Scheme 6

although 4–30 times smaller than the photoinduced process.[34] Obviously, this work is expected to attract much interest, mainly aimed at the optimisation of the electron donor ability of the zeolite framework and the development of a practical application of this finding in the field of photocatalysis. For instance, it can be easily anticipated that zeolites containing heteroatoms such as Ge, Ti could improve the yield of this pumping system. Also these electrons could serve to generate superoxide or other aggressive oxygen species capable to initiate degradation of organic pollutants.

Kincaid has developed a more sophisticated synthetic strategy in which by using 2,2′-bipyrimidine or 2,3-bis(2-pyridyl)pyrazine as a ligand, he has been able to develop a spatially organized photocatalytic system containing two slightly different ruthenium(II) polypyridyl complexes such as bis(2,2′-bipyridyl)(2,2′-bipyrazinyl)ruthenium(II) (E° 1.50 V) and tris(5-methyl-2,2′-bipiridyl)ruthenium(II) (E° 1.18 V), in neighbour supercages.[35,36] Upon irradiation, the vectorial electron transfer from the complex with the higher potential to the neighbour complex with lower potential and then to viologen produces an unprecedently efficient charge separation as consequence of the long distance between the charge separated species, minimizing the energy-wasting back electron transfer.[37]

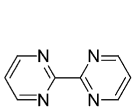

2,2'-bipyrimidine

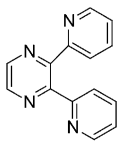

2,3-bis(2-pyridyl)pyrazine

Further work on the use of zeolite encapsulated $Ru(bpy)_3^{2+}$ in combination with TiO_2 will be commented upon in the section devoted to zeolites encapsulating clusters of titanium dioxide.

Besides ruthenium trisbipyridyl complex, metallophthalocyanines can also act as electron donors upon photochemical excitation. Mechanical mixtures of metallophthalocyanines and zeolites have been found effective for the photocatalytic degradation of model compounds representing the major components of petroleum hydrocarbons.[38] The degradation order with this photocatalyst follows the order aromatics > naphthenes > paraffins. Crude oil photodegradation has also been examined with these phthalocyanine/zeolite mixtures.[38] Given that metallophthalocyanines are among the first metallic complexes encapsulated inside zeolites by ship-in-a-bottle synthesis and that they can also be prepared by build-the-bottle-around-the-ship,[21,22,39] it would be of interest to investigate these zeolite-occluded dyes as photocatalysts as they have been studied as heterogeneous oxidation catalysts.[23,25,40]

2,4,6-Triphenylpyrylium encapsulated within zeolites as electron acceptor photosensitisers

Tetrafluoroborate, perchlorate, hydrogen sulfate and other salts of 2,4,6-triphenylpyrylium (TP^+) are powerful electron acceptor photosensitisers in solution.[41] As solvents, acetonitrile, dichloromethane and ethanol can dissolve these salts of TP^+ and they have been used as media in these photosensitised reactions. TP^+ becomes a very strong electron acceptor upon excitation. Its oxidation potential has been estimated to be ~2.5 and ~2.0 V *vs.* SCE for the singlet and triplet excited state, respectively.[41] This remarkable oxidizing power makes TP^+ salts of general applicability as electron transfer photosensitisers for a wide range of chemical structures including aromatics and alkylaromatics, dienes and alkenes, epoxides, strained hydrocarbons, *etc.*[41] Miranda and Garcia have reviewed the photoinduced electron transfer reactions promoted by TP^+ photosensitization in solution. Unfortunately, pyrylium ions are not stable in aqueous solutions at neutral pH. In this reaction, pyrylium ions are subject to hydrolytic ring opening. This thermal instability precludes the use of TP^+ as photosensitisers in water.

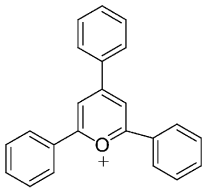

TP^+

In this regard, the encapsulation by ship-in-a-bottle synthesis of this large heterocyclic cation inside the supercages of zeolite Y enhances remarkably the thermal and photochemical stability of this photosensitiser.[42] Initially the synthesis of TP@Y[43] was achieved by reacting acetophenone with two equivalents of chalcone using the Brønsted acid sites of HY zeolites as catalyst (Scheme 7). This reaction to form TP^+ mimics a preparation

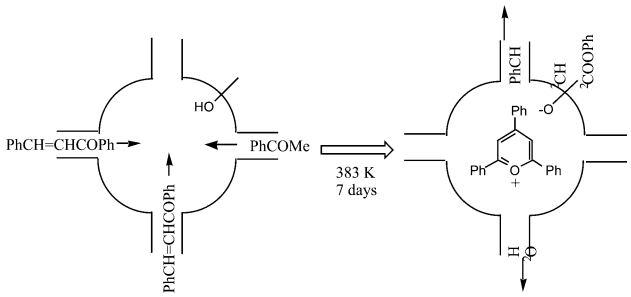

Scheme 7 Preparation procedure followed to obtain TP@Y.

procedure in solution.[42] However, it suffers from the disadvantage of low reproducibility depending on the overall acid strength and the acid site distribution of each actual HY batch and the need of subsequent neutralization of the residual acid sites when the non-acidic Na^+-form of the TP@Y is the desired photocatalyst.

More recently, Miranda, Braun and co-workers have reported a simplified synthesis of TP@Y in which starting from commercially available materials, the experimental procedure simply consists in stirring at room temperature an aqueous suspension of commercial $(TP)HSO_4$ and commercial NaY at neutral pH.[44] The mechanism involves the *in situ* opening of the heterocyclic ring to form the 1,3,5-triphenyl-2-penten-1,5-dione that subsequently is adsorbed into the zeolite (Scheme 8). The process is finished by baking at moderate temperatures (< 200 °C) the zeolite containing the pentendione to produce the thermal cyclization and formation of the heterocycle. The whole process just requires stirring a suspension and baking to obtain high-quality TP@Y. Moreover, the TP^+ loading can be easily controlled by varying the $(TP)HSO_4$/NaY

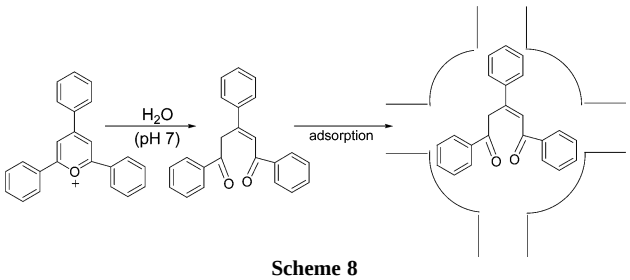

Scheme 8

ratio. Samples containing above 15 wt% of TP^+ can be obtained, while these high loadings were not achievable by the earlier aldolic condensation procedure.

TP^+ ion can be supported on silica, MCM-41 and other inorganic oxides or high surface area solids. In these cases, the preparation procedure is even simpler since these solids can be obtained by adsorbing a soluble salt of TP^+ such as BF_4^-, HSO_4^- or ClO_4^- from a solution on the solid. TP^+ is deposited on the external solid surface of amorphous oxides or in the large mesopores of structured silicates, the molecular size of TP^+ being no problem for these systems. TP^+ when supported on the external surface or in large mesopores exhibits the highest intrinsic photocatalytic activity at initial time, as for instance in the photochemical *cis–trans* isomerisation of stilbene as a model reaction.[45] This activity can be even higher than that of the same or analogous soluble salts in solution.

Encapsulation inside the micropores of zeolites reduces considerably this initial photocatalytic activity (measured as the slope at zero time of the plot of degradation percentage *versus* the irradiation time) due to diffusion restrictions through the zeolite micropores, making it more difficult for the substrate to reach the immobilized photosensitiser. However, encapsulation inside the micropores of zeolites renders TP^+ indefinitely persistent towards hydrolysis in water at room temperature and neutral pH. Even upon illumination TP@zeolite is photostable and generates a stationary concentration of H_2O_2. In contrast, TP^+ supported on SiO_2 or MCM-41 undergoes hydrolysis, this limiting their use in water to very short irradiation times and making these systems not reusable. As result, the final productivity, defined as the mass of substrate reacted per mass unit of photocatalyst, can be significantly higher when TP^+ is encapsulated in zeolites than when deposited on the surface of silica or MCM-41.

Illumination of aqueous suspensions of TP@zeolite generates $OH^\cdot$ hydroxyl radicals. This has been demonstrated by the formation of hydrogen peroxide, detection by laser flash photolysis benzene and methyl viologen adducts of $OH^\cdot$, detection by EPR of $OH^\cdot$ adduct of the pyrrolidine N-oxide derivatives and by means of product studies. Photocatalytic generation of hydroxyl radicals without self-degradation is the key feature for the application of TP@zeolite as photocatalyst in aqueous solution.

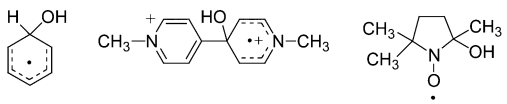

benzene-OH adduct viologen-OH adduct pyrrolidine-OH adduct

The ability of the TP@zeolite photocatalysts to generate upon illumination a stationary concentration of hydrogen peroxide (in the range 10^{-2}–10^{-3} M) can be utilized to promote catalytic oxidations. Thus, Corma and García have prepared a bifunctional photocatalyst in which TP^+ has been encapsulated in a (Ti)Beta zeolite.[46] The crystalline titanosilicates, and in particular (Ti)Beta, exhibit a high catalytic activity towards the epoxidation of alkenes with hydrogen peroxide.[47] The idea was to couple the ability of TP@Y to generate hydrogen peroxide by irradiation with the catalytic activity of (Ti)Beta to promote epoxidation of alkenes. In this way, irradiations of cyclohexene in acetonitrile–water slurries

of TP@(Ti)Beta form significant concentrations of cyclohexanediol, thus, demonstrating this principle. It would be worth expanding this methodology to prepare other bifunctional, photo- plus thermal-, catalytic systems, the difficulty here being the low photo-stationary concentration of H_2O_2.

TP@Y is able to effect the degradation of a series of pesticides widely-used in agriculture such as insecticides, acaricides and herbicides. After being sprayed in the field these pesticides are normally encountered in surface waters. The concentration of these pesticides in water may be particularly large in agricultural areas and during the corresponding season.

Thus, TP@Y has been found more active than P-25 TiO_2 standard for the solar light degradation of 4-chlorophenoxyacetic acid.[48] The latter aryloxyacetic acid is a model for widely-used polychlorinated 2T and 3T herbicides. Cl^- was found to be formed in the mineralisation process. The photocatalytic activity of TP@Y is also higher than that of other dye-encapsulated photocatalysts such as malachite green encapsulated within zeolite Y. Apparently the higher match of the absorption spectrum of TP^+ with the solar emission spectrum at the Earth surface, together with the higher electron acceptor ability of TP^+ are the factors responsible for this higher activity.[48] The zeolite framework in co-operating to the photocatalysis by adsorbing strongly the herbicide within the pores favouring its close contact with the photosensitiser. Physical adsorption of the pesticide inside the pores is a process much faster than the actual photodegration that requires longer times to take place to a significant extent.

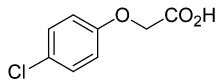

4-chlorophenoxyacetic acid

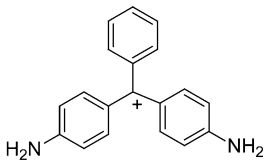

malachite green

Also in this context, propoxur commercialised under the trade mark of *Baygon* is a common insecticide. A photochemical study has demonstrated[49] that while direct irradiation of propoxur with medium pressure mercury lamps through quartz (most intense wavelength at λ = 254 nm) produces among other photoproducts the photo-Fries hydroxyarylcarboxamide isomers with only a 16% of mineralisation (measured as the decrease in the total carbon content of irradiated aqueous solutions containing propoxur), irradiation through Pyrex (λ > 300 nm) leaves propoxur absolutely unaltered. However, addition of TP@Y produces for the same irradiation time a considerably higher mineralisation (50% of total carbon content decrease) upon irradiation with light of λ > 300 nm, that are wavelengths more similar to the solar light emission spectrum. The photocatalytic generation of nitrate ion from mineralisation of the N atoms (7% of the initial propoxur concentration) was also determined by ion chromatography in the irradiation mixture. Under the same conditions (λ > 300 nm), the use of the same weight of P-25 TiO_2 as photocatalyst gives somewhat higher (70%) mineralisation levels.

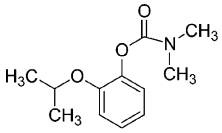

propoxur

Novel photocatalysts based on pyrylium derivatives

The search for more efficient pyrylium-based photocatalysts has led to the ship-in-a-bottle synthesis of related dyes. For example a tetraphenylbipyrylium cation, that has to be accommodated in two neighbour supercages due to its large molecular size (Fig. 1), has been synthesized starting from terephthaldehyde and acetophenone in the presence of HY zeolite.

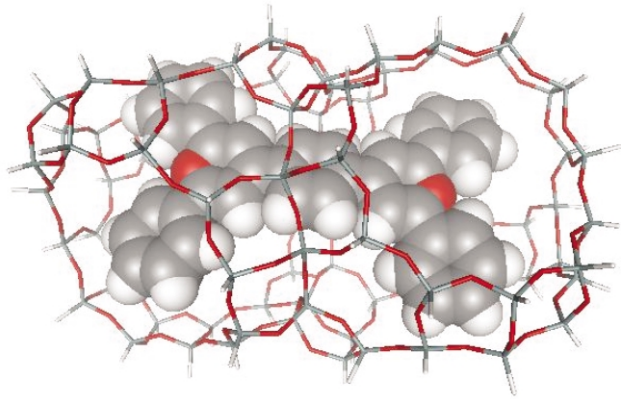

Fig. 1 Visualization of the best docking of optimisated tetraphenylbipyrylium within two neighbour supercages of an idealized all-silica Y zeolite.

Although in this particular case the photocatalytic activity of the zeolite comprising the encapsulated bipyrylium is lower than that of TP^+, a new generation of more active photocatalysts has been developed based on 2,4,6-triphenylthiapyrylium ($TPTP^+$) rather than TP^+.[50] Perchlorate and other inorganic salts of $TPTP^+$ are more stable than the TP^+ analogs due to the higher aromaticity of $TPTP^+$ arising from the similar electronegativity of C and S as opposed to the pyrylium where the positive charge is more localized on the oxygen atom.[50]

Energy transfer photosensitization

There are some cases in which the photosensitiser absorbs light and upon reaching an electronic excited state it is able to transfer this energy to a substrate that becomes electronically excited even if the substrate has not directly absorbed the light. Given the relative lifetime of singlet and triplet excited states, energy transfer photosensitization is more common for longer-lived triplet excited states (Scheme 9). Singlet excited states living typically nanoseconds are much too short lived to efficiently allow energy transfer, while triplets are several orders of magnitude longer lived.

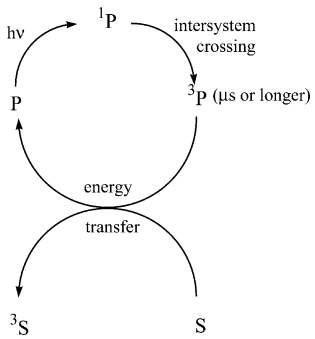

Scheme 9

On the other hand, for those molecules for which the triplet excited state cannot be directly populated due to the low efficiency of intersystem crossing, energy transfer photosensitization can serve as an alternative to generate those excited states. The photosensitiser for triplet energy transfer has to meet two conditions, namely, long wavelength light absorption to avoid direct excitation of the substrate and a highly efficient intersystem crossing. Aromatic ketones and in particular benzophenones and xanthones, are among the most widely used energy transfer photosensitizers.[51,52]

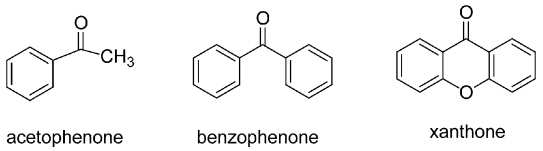

In order to obtain a truly heterogeneous energy transfer photocatalyst, 4-amino benzophenone has been adsorbed on acid zeolites.[53] It was hoped that an acid–base reaction will anchor the weakly basic 4-aminobenzophenone by protonation of the $-NH_2$ group providing an ionic bond to the solid (Scheme 10).

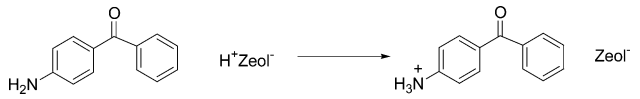

Scheme 10

1,3-Cyclohexadiene dimerisation has been proposed as a test reaction in which it is possible to distinguish between energy transfer and electron transfer mechanisms by simple analysis of the product distribution (Scheme 11).[54,55] Pure energy transfer gives

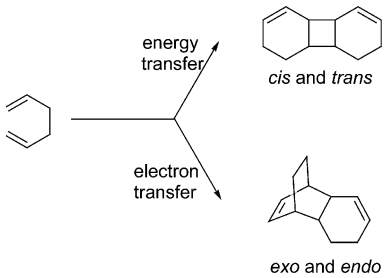

Scheme 11

rise to [2+2] cycloadducts, while electron transfer mediated dimerisation leads to [4+2] dimers. Acid catalysis does not effect cyclodimerisation. By means of 1,3-cyclohexadiene dimerisation as a test reaction, it has been demonstrated that adsorption of 4-aminobenzophenone into acid zeolites does not produce clean energy transfer photosensitizers, but a series of solid photosensitizers that act through a combination of energy and electron transfer in different proportions depending on the acid strength of the zeolite. Thus, protonation and zeolite encapsulation enhance the electron acceptor ability of a typical energy transfer benzophenone. This behaviour is not totally unexpected in view of the fact that after protonation the electron deficiency of the *para*-phenylene ring has considerably increased and of the high micropolarity of the zeolite cavities.

Among the advantages of photosensitiser encapsulation, one that has been rarely exploited is the possibility to introduce shape-selectivity. This effect, well established in thermal catalysis by zeolites,[56–58] consists in modifying the product distribution observed in solution merely by geometrical constraints arising from the different shape and molecular size of reagents, products and transition states. Those molecules whose dimensions allow diffusion within the pores of the zeolite can react with the internal active sites, while those others whose size is too big to permit access to the interior of the pores cannot react. In shape-selective catalysis, the only reason why the product distribution is altered with respect to that found in solution is by the different molecular geometry. One example of shape-selective photocatalysis is the one-way photoisomerisation of *trans*-stilbene to the *cis* isomer. Zeolite ZSM-5 (5.2 × 5.4 Å) permits the access of the *trans* configured stilbene, while the *cis* isomer is too large to enter the pores. Thus, by using 4-aminobenzophenone encapsulated within zeolite ZSM-5, photostationary mixtures much enriched with the *cis*-stilbene are obtained in comparison with the behaviour of this photosensitiser in solution (Scheme 12).[59] Another example of shape-selective photocatalysis using ETS-10 will be commented on later in the section on photocatalytically active framework zeolites.

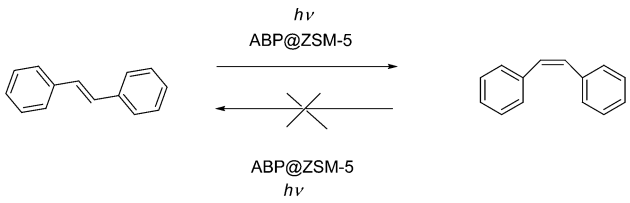

ABP: 4-aminobenzophenone

Scheme 12

Besides 4-aminobenzophenone, the same idea of using an acid zeolite to anchor ionically a photosensitiser containing a basic amino group has been later used by Ramamurthy *et al.* to obtain 4-aminoacetophenone-doped zeolite Y.[60]

One special type of energy transfer photosensitizer of general importance that will be discussed in the next section are those able to generate singlet oxygen.

Singlet oxygen photocatalysts

Oxygen constitutes a rare case, since the ground electronic state of this molecule is a triplet, while almost all ground states of molecules are singlets. Energy transfer with spin inversion is a very simple way to generate one of the electronically excited singlet states of oxygen, rendering this molecule considerably more reactive.[61] This energy transfer is normally accomplished by photoexcitation of a singlet oxygen photosensitizer. Singlet oxygen reacts rapidly with alkenes and aromatic hydrocarbons, the *ene* reaction and cycloadditions being two of the most general reactions (Scheme 13). The major problem in singlet oxygen reactions is the lack of selectivity of this highly reactive molecule.[62]

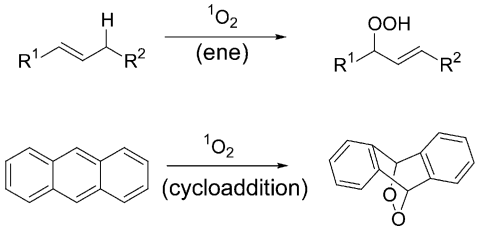

Scheme 13

Thionin, methylene blue or methylene green are singlet oxygen photosensitizers that have been adsorbed within zeolites X and Y with the aim of controlling the selectivity of singlet oxygen *ene* reactions. Encapsulation of these dyes at 1 molecule of sensitiser per 100 supercages minimizes the tendency of these dyes to aggregate and to undergo self-quenching, thus, apparently enhancing the singlet oxygen generation quantum yield. Clennan has recently published a critical account of the state of the art in the use of zeolite supported photocatalysts for singlet oxygen oxygenation and the reader should refer to this review for an in-depth discussion on this subject.[63] By studying the photooxygenations of a series of tetrasubstituted alkenes in methylene blue-doped zeolite Y, Clennan and Sram suggested[64] a model to rationalize the regioselectivity of singlet oxygen *ene* reactions using zeolite-bound photosensitizer in which the alkene forms a complex with the alkali metal ions present in the zeolite supercage forcing the allylic methyl groups to occupy the face of the olefin approached by the singlet oxygen (Scheme 14). As the singlet oxygen approaches to the alkene and starts forming a perepoxide intermediate the alkali ion shifts a little to stabilize electrostatically this intermediate. Steric interactions in these alkali metal ion-perepoxides govern the population of each diastereomer and electronic interactions dictate the regioselectivity of perepoxide opening.

Photosensitised singlet oxygen *ene* reactions using zeolite encapsulated photocatalysts have synthetic potential since the regioselectivity that is observed using photosensitizer-doped NaY

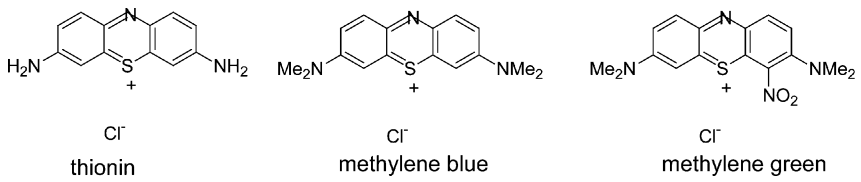

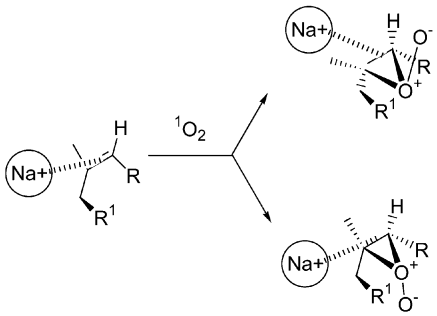

Scheme 14

cannot be obtained by other means. Stratakis and co-workers have reported excellent selectivity towards the formation of a single regioisomer of allylic hydroperoxide (Table 1).[65–67] However,

Table 1 Results of the singlet oxygen *ene* reaction of alkenes in the presence of thionin doped NaY

Substrate	Products (%)	
Zeolite	Exclusive product	
Solution	53	47
Zeolite	6	94

attention has to be paid to the mass balance in which the products are obtained and the substrate-to-photocatalyst weight ratios employed. In some cases, the amount of substrate oxidized is so small (~ 5 mg)[68] that the results may be affected by large errors.

Zeolites encapsulating clusters of semiconductor oxides

Titanium dioxide

Transition metal oxide photocatalysts, including titanium, vanadium and chromium oxides, can be incorporated into the cavities and framework of various zeolites and mesoporous molecular sieves either by ion exchange or during the hydrothermal synthesis. For the introduction of titanium oxide clusters, one possibility is the ion exchange in aqueous medium using mixed oxalate salts such as $(NH_4)_2(Ti{=}O)(C_2O_4)_2$.[69,70] Another alternative to obtain quantum-sized TiO_2 clusters encapsulated within zeolites starts with the adsorption of titanium tetraisopropoxide within the zeolite in isopropyl alcohol containing citric acid followed by addition of ethylene glycol to obtain uniformly dispersed TiO_2 nanoclusters.[71] The materials prepared may contain initially highly dispersed anchored transition metal oxide species in tetrahedral coordination, the hallmark of titanium isolation being a blue shift of the absorption onset with respect to that of bulk anatase.[70] Also the observation of photoluminescence can be considered a characteristic of nanoscopic TiO_2 clusters as opposed to non-luminescent bulk anatase or rutile.[72]

TiO_2 clusters inside zeolites are able to effect interfacial electron transfer such as the photochemical reduction of methyl viologen to the corresponding radical cation.[70] More interesting from the photocatalytic point of view, zeolites incorporating TiO_2 clusters may act as efficient photocatalysts for the decomposition of NO into N_2 and O_2, for the efficient removal of ammonia and hydrogen sulfide from air and the reduction of CO_2 with H_2O. Also in the liquid phase, these zeolites containing titania can also effect the degradation of organic material in waste waters.

By analogy with pure oxides, it is generally assumed that the photochemical activity arises from the ligand-to-metal charge transfer excited state, *i.e.*, a photoinduced single electron transfer from the $O^{=}$ considered as a ligand to the titanium(IV) atom. Photoluminescence studies,[72] when photoluminescence is observed, can serve to determine the efficiency of generation and lifetime of this charge separated state, and even to demonstrate the interaction of these chromophores with the decomposing reactant, particularly for gaseous substrates. Zeolites and mesoporous molecular sieves provide to these photocatalytic systems their uniqueness in terms of pore size, crystal structure, internal location of ions and adsorption capability that can modify and enhance the efficiency of the photocatalytic process.[73] The crystal structure of the zeolite can determine the size of the encapsulated TiO_2 clusters and, therefore, their bandgap and the onset of their optical absorption.[74]

Anpo and co-workers have been extremely active in this area of zeolite-encapsulated semiconductor oxide photocatalysts. Among the reactions that have attracted more attention, one is the photocatalytic reduction of CO_2 by H_2O. The reaction resembles the photosynthesis effected by green plants. No doubt that this photochemical reaction leading to CO_2 fixation will become an industrial process if the inherent technical problems associated with photocatalysis and photocatalytic reactors were solved. This photochemical reaction has been studied in the presence of a series of zeolites and mesoporous molecular sieves containing encapsulated TiO_2 clusters or framework Ti atoms at 45 °C leading to the formation of CH_4, CH_3OH along with minor concentration of CO and O_2.[75,76] Isolated tetrahedrally coordinated titanium oxide highly dispersed within the zeolite frameworks exhibited a high selectivity towards CH_3OH formation, that is closely related to the concentration of charge transfer triplet ($\equiv Ti^{3+}$-$O^{\cdot}$-) excited state. The selectivity for methanol formation also depends on the hydrophobic/hydrophilic properties of the photocatalyst.[75,77] The highly dispersed titanium dioxide species encapsulated within the zeolite cavities exhibit high photocatalytic activity due to the high reactivities of their charge transfer excited states, the main problem

being to expand its photoresponse from short wavelengths in the UV towards the visible light.[73] Doping with Cr or V can modify the electronic states of doped TiO_2, resulting in the shift of the absorption onset to longer wavelengths.

Due to its isoelectric point, TiO_2 particles form complexes easily with organic carboxylic acids that bind electrostatically as carboxylate to the positive surface of TiO_2. TiO_2 clusters encapsulated within zeolite Y also behave similarly. Yoon and Kim have recently reported that TiO_2@Y forms a charge transfer complex with *p-N,N*-dimethylaminobenzoic acid.[78] Dimethylaminobenzoic acid bound to titania clusters encapsulated within zeolites exhibits dual emission from aminobenzoic localized excited state and from the aminobenzoic-titania charge-transfer complex. The latter emission in TiO_2@Y is very weak as compared to the intensity of the same emission in solution or in other heterogeneous systems. This effect has been attributed to the occurrence for the zeolite Y encapsulated TiO_2-aminobenzoic complex of an efficient electron injection from the carboxylic acid excited state to the conduction band of TiO_2 in the zeolite. The conduction band electron of TiO_2 is claimed to be also transported through the zeolite framework and the system has been used to effect the photocatalytic reduction of methyl orange in water with a quantum efficiency of 0.34 that is a very high value (Scheme 15).

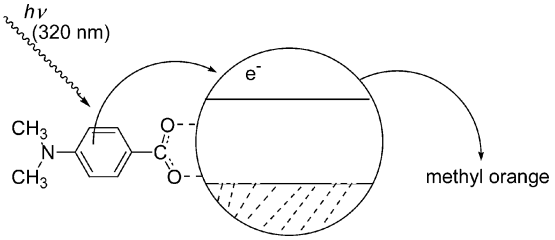

Scheme 15

Surprisingly dimethylaminobenzoic acid is only marginally decomposed in the photocatalytic processes.

Concerning the application in photocatalysis, the simplest system consists in the use of mechanical mixtures of TiO_2 and zeolites as photocatalysts. These solid mixtures have been applied to the treatment of air, gas, water and liquids using visible or solar light.[79,80] Mechanical mixtures of TiO_2 (as photocatalyst) and zeolites (as adsorbents) after being submitted to sintering processes using suitable binders are simple but efficient filters to effect the photocatalytic deodorization of polluted air as well as for air purification and disinfection.[81–97] The TiO_2-zeolite photocatalyst can be placed on a monolith having a honeycomb configuration[98,99] or a membrane[94,100] to facilitate the gas flow through the system and ensure the exposure to the light.[101,102]

One simple preparation procedure consists in dipping an inert glass fiber support into a zeolite sol–gel suspension containing a dispersion of the photocatalyst or its precursor, followed by baking it at high temperature.[103] The zeolite to be mixed with TiO_2 may be ion exchanged and contain Ag, Cu or any other combination of transition metals.[104] Sometimes the mixture of TiO_2 and zeolites are supported on polysiloxane membranes or porous resin films of PFTE.[105,106] These fluorous resins can be conveniently modified by introducing OH and/or CO_2H to facilitate the adsorption of the photocatalyst.[107]

Volatile aldehydes and carboxylic acids, ammonia and amines as well as organic sulfur-containing compounds are the target compounds to be decomposed from air. Photocatalytic degradation of propionaldehyde over TiO_2 loaded on zeolites as adsorbents has been studied and observed that the CO_2 evolution correlates well with the apparent diffusion coefficients of propionaldehyde on the various zeolites and adsorbents.[108] These systems can be used for the deodorization of refrigeration equipment.[101,102]

Likewise, an ethylene-decomposing apparatus based on the combination of TiO_2 and zeolite can be used in chambers for vegetable and fruit storage.[109,110] Some vegetables and fruits emit ethylene whose presence in the air is undesirable since it promotes aging and ripening effects.

Also noxious NO_x can be removed from air by preparing films from suspensions containing zeolites particles and TiO_2 fine particles. These films are deposited on fibers of inorganic fibrous supports and constitute the active photocatalytic layer of the plates.[111,112]

Mechanical mixtures of TiO_2 and zeolites have also been claimed to be efficient systems for disinfection of bath and swimming pools,[113,114] as well as for water purification in fish tanks and aquariums.[115] A networks of patents have also covered the application of mixtures of TiO_2-zeolites deposited on polyester fibers for the preparation of durable, odor-proof and antibacterial fabrics.[116–120] Mixtures of TiO_2 and zeolites have also used as herbicides to inhibit weed growth.[121]

Concerning the co-operation of TiO_2 particles and zeolites as photocatalysts, an interesting study has focused on the photocatalytic oxidation ($\lambda > 300$ nm) of alkylbenzenes to α-ketones and of alkenylbenzenes to epoxides and ketones arising from oxidative C=C degradation.[122] Compared to TiO_2, addition of acid zeolites increases or decreases the oxidation rate depending on the substrate, but it increases in all cases the selectivity towards the oxidation product.

A more elaborated photocatalyst for the decomposition of NOx consists in the encapsulation of TiO_2 clusters inside the zeolite voids. Anpo and co-workers have found that zeolites with low Si/Al ratio are more suitable for encapsulating TiO_2 through the exchange or impregnation methodology, exhibiting a high and unique activity for the photocatalytic decomposition of NO to N_2 and O_2 at 2 °C.[123] Chemical vapour deposition has also been used to prepare Ti oxide and V oxide incorporated inside the zeolite micropores.[124] Diffuse reflectance UV absorption, photoluminescence and XAFS indicate that the Ti oxide species are highly dispersed within the zeolite and exist in tetrahedral coordination. The charge transfer excited state of these highly dispersed Ti oxide are proposed to be responsible for this efficient NO photocatalytic decomposition. It was demonstrated that aggregates of octahedrally coordinated Ti oxide shows a different photocatalytic activity.[125]

Garcia and Scaiano have prepared a series of photocatalysts based on the inclusion of TiO_2 clusters on zeolites of different crystal structure and observed variations in the optical spectra that have been interpreted as indicating the operation of quantum size effects due to the control of the zeolite framework on the size and shape of the incorporated TiO_2 clusters. The relative photoactivity of these TiO_2@zeolite photocatalysts for the photooxygenation of thianthrene as a model compound was tested.[74]

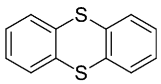

thianthrene

TiO_2 in zeolites have also been used as photocatalysts for the treatment of CN^- containing waste waters.[126] In this case UV irradiation results in CN^- removals of 90% at initial CN^- concentrations of 2.6 ppm and a pH value of 13.[126] Upon deactivation, the photocatalyst efficiency can be restored by flushing with distilled water.

An interesting application worth pursuing is the photosplitting of water. Zeolites containing TiO_2 aggregates in combination with a noble metals such as Pt or Pd have been tested for the photosplitting of water to form hydrogen.[127,128] In a series of pioneering works,[129–131] Mallouk and co-workers designed a multicomponent system spatially arranged in zeolite L that is able to generate H_2 from water by irradiation in the presence of sacrificial amines as electron donors. These systems contain an organic dye to harvest light, TiO_2 nanoparticles as electron relays, internal methyl

viologen to act as electron sinks and a noble metal to catalyse H_2 evolution (Scheme 16).

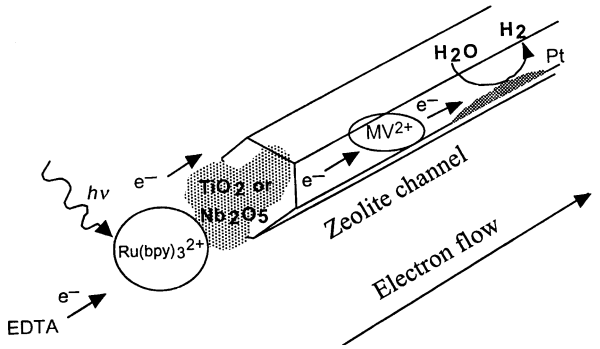

Scheme 16

Titanium dioxide aggregates have also been included within the channels of MCM-41 and FSM-16 by reacting $TiCl_4$ in hexanes with the as-synthesized mesostructured silicate.[132] The solids have been characterized by an extensive array of surface techniques including powder XRD, TEM, SEM, XPS, N_2 adsorption, solid state ^{1}N NMR, IR and UV-Vis spectroscopy. The conclusion from the characterization is that the materials contain well-dispersed $(TiO_2)_n$ clusters (n ranging between 30 and 70) included within the channels of the mesoporous silicates.[132] These clusters are covalently attached to the silicate walls through Si–O–Ti bonds. Some minor anatase TiO_2 particles of size between 10–25 nm were sometimes observed. These mesoporous systems are certainly interesting since they can overcome certain limitations of the TiO_2-supported zeolites in terms of Ti loading and substrate diffusion. The titania-grafted MCM-41 sample exhibits high catalytic activity for the photobleaching of rhodamine–6G or the oxidation of α-terpineol.[132]

Bossmann and Braun were the first to publish a two-component system comprised of $Ru(bpy)_3^{2+}$ and TiO_2 clusters inside zeolite Y.[133,134] The $[Ru(bpy)_3^{2+}$–$TiO_2]$@Y solid was characterized by elemental analyses, optical spectroscopy, electrochemistry and transmission and raster electron microscopy.[133] Shortly after this report and independently, the photophysics of this $[Ru(bpy)_3^{2+}$–$TiO_2]$@Y system was studied by time-resolved emission and laser flash photolysis.[135] In this bi-component system, the ruthenium complex acts as sensitiser absorbing visible light and transferring electrons to the TiO_2 clusters that would act as electron relay.[133,135] This system is reminiscent of those employed in solar cells based on ruthenium dye-sensitised porous TiO_2.[136]

Bossmann and Braun demonstrate that photoexcitation produces the vectorial electron transfer from entrapped $Ru(bpy)_3^{2+}$ in its excited-state towards size-excluded trisphenanthrolyl Co(III) complex, the efficiency of the electron transfer increasing with the loading of TiO_2.[133] These TiO_2 clusters act as electron relays from the internally located electron donor to the external Co(III) complex. The $[Ru(bpy)_3^{2+}$–$TiO_2]$@Y photocatalyst exhibits an enhanced activity towards the degradation of 2,4-xylidine in the presence of hydrogen peroxide as compared to $Ru(bpy)_3^{2+}$@Y photocatalyst. It can even be active with solar light.[134]

Analogously, a comparison of the photocatalytic activity of $Ru(bpy)_3^{2+}$@Y and that of $[Ru(bpy)_3^{2+}$–$TiO_2]$@Y for the deactivation of horseradish peroxidase has observed a synergistic effect of the mediated enzyme deactivation due to the presence of the TiO_2 (Fig. 2).[135]

A further elaboration of this multi-component $[Ru(bpy)_3^{2+}$–$TiO_2]$@Y photocatalyst consists in the co-incorporation of Pt in the system. This multicomponent system has also been reported by Bossmann and Braun.[137] They have demonstrated that upon irradiation with a medium-pressure mercury lamp this $[Ru(bpy)_3^{2+}$–$TiO_2]$@Y photocatalyst incorporating Pt is able to effect the photodegradation of 2,4-xylidine to carbon dioxide and

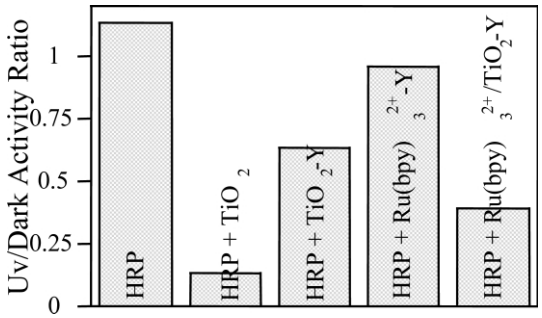

Fig. 2 Relative enzymatic activity measured for horseradish peroxidase (HRP, blank activity under the same conditions in the dark) in water and upon irradiation (λ 355 nm) in the presence of different photocatalysts. TiO_2 corresponds to Degussa P-25. (Figure taken from ref. 135. Reproduced with permission from *J. Phys. Chem. B*, 2002, **106**, 2460. Copyright 2002, American Chemical Society.)

the concurrent reduction of water to dihydrogen. The presence of Pt acts as efficient catalytic site for the evolution of H_2. This three-component system assembled in zeolite is reminiscent of those commented upon earlier developed by Mallouk for the photogeneration of hydrogen except that the sacrificial electron donor is an undesirable pollutant.[131,138] The quantum yield of this process has been estimated to be 0.08 ± 0.001 for polychromatic irradiation.[137] Clearly these studies are worth continuing since the coupling of the photodegradation of pollutants with the generation of clean fuels is a very interesting approach to accomplish two targets conveniently.

Vanadium oxide and other semiconductors

Pure or supported vanadium oxides exhibit high photocatalytic activity for many reactions, particularly important being alkane oxidation and CO_2 fixation.[47] The photocatalytic efficiency of vanadium oxides is even higher than that of titanium oxides, with the additional advantage of having absorption bands in the visible region. The actual absorption spectrum of vanadium containing solids depends on vanadium oxidation state, but it is not uncommon to have an onset above 400 nm (yellow colour). Vanadium oxide can be easily grafted on the surface of metal oxides, the level of dispersion and the nature of the sites being a function of the vanadium loading and the nature of the oxide support (Scheme 17).

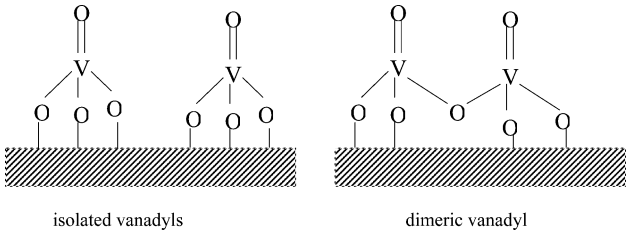

Scheme 17

The distribution of the vanadium in the different possible species has been addressed by a combination of different spectroscopic techniques including optical spectroscopy, Raman, ^{51}V NMR, EPR and XAFS. The presence of vanadyl V=O groups as well as single V–O bonds and dimeric or oligomeric vanadium species has been established.

Supported vanadium oxides have attracted much interest due mainly to their activity as thermal catalysts in the gas-phase oxidation, dehydrogenation, oxydehydrogenation and lateral chain oxidation of alkyl aromatics.[47] Some of these reactions can be equally promoted photochemically, of particular importance being the photoxygenation of methane, ethane and light alkanes.

Vanadium can be supported on inorganic oxides in several ways, a common one being the reaction of vanadyl chloride ($VOCl_3$) or any other reactive species. Alternatively, chemical vapour deposition or baking vanadium oxides with other inorganic oxide supports

can also be viable procedures for grafting vanadyl on supports. A general problem with supported vanadium oxides that severely limits their applicability is, however, their tendency to undergo vanadium leaching upon prolonged contact of the solid with liquids. Leaching causes not only depletion of the vanadium content of the photocatalyst, but more importantly, generates a homogeneous photochemical process competing with the derived heterogeneous process. Leaching can occur to a large extent especially in water due to the solubility of vanadium oxides in water at certain pHs, thus, impeding the applicability of vanadium photocatalysts to waste water treatment. It can be said that any vanadium supported oxide has to be extensively surveyed for vanadium leaching before accepting as truly heterogeneous a process in which a vanadium supported photocatalyst is used. Vanadium containing photocatalysts other than those in which vanadium forms part of the molecular sieve or is included within the voids of the porous host will not be covered in the present review.

As described above for titanyl groups, vanadyl can also be ion exchanged in zeolites as a monomeric precursor of entrapped vanadium oxides or, alternatively, solids in which vanadium occupies framework positions in molecular sieves can be synthesized by hydrothermal crystallization. This is the case of crystalline AlPOs, which can be obtained having vanadium in framework positions (VAPOs). However, in VAPOs vanadium can easily migrate from framework to out-of-framework positions, also rendering these solids prone to vanadium leaching when contacted with water and other liquids. Nevertheless, these vanadium-containing solids can serve as photocatalysts for gas-phase reactions such as the decomposition of NO or the photocatalytic reduction of CO_2 with H_2O to form CH_3OH and CH_4.[123]

Photocatalysts based on the incorporation of other semiconductors within zeolites have also been reported. Thus, ZnO has been encapsulated in sodalite. EXAFS and X-ray emission indicate that Zn is in tetrahedral positions inside the sodalite cage.[139] ZnS and CdS encapsulated within zeolites A, Y and E have been prepared by sulfidation with H_2S at 400 °C of Zn^{2+} or Cd^{2+} ion exchanged samples.[140] Optical and emission spectroscopies indicate that the samples exhibit quantum size effects, minor variations in the cluster size being reflected in the semiconductor bandgap and the absorption onset of the optical spectrum. In this respect, TiO_2 is the worst case to observe quantum size effects since the particle size below which these effects appear in TiO_2 is only a few nanometers. In contrast, CdS is the archetypical semiconductor for quantum size studies.

CdS@zeolite has been reported as photocatalysts for the splitting of water, generating hydrogen in the presence of suitable sacrificial donors.[140] It was observed that for zeolite Y the photocatalytic efficiency increases when the CdS@Y is co-doped with ZnS, the maximum efficiency being achieved at a Cd/Zn ratio of 0.25. It has been proposed that these optimised materials are organized in such a way that the CdS nanoparticles are located in the α-cages and ZnS clusters in the larger β-cages.

Photo-Fenton processes

Fenton reaction of hydrogen peroxide with Fe(II) species is known to produce stoichiometric amounts of hydroxyl radical according to eqn. (1). As mentioned earlier hydroxyl radical is among the most aggressive species that can be generated in water and attacks virtually any organic molecule present in the medium. This attack is the initial step yielding oxidized products and after consecutive ·OH attack/oxidation cycles may eventually lead to mineralisation of the organic material present in water.

$$Fe^{2+} + H\text{–}OO\text{–}H \rightarrow Fe(OH)^{2+} + {\cdot}OH \quad (1)$$

An alternative to the use of stoichiometric amounts of iron salt is the photo-Fenton reaction, in where eqn. (1) is coupled with the subsequent photochemical reduction of aquated Fe(III) species back to the Fenton active Fe(II).[141–143] Moreover, this reduction also produces additional concentrations of ·OH radicals as indicated in eqn. (2).

$$Fe^{3+} + H_2O \xrightarrow{h\nu} Fe^{2+} + H^+ + {\cdot}OH \quad (2)$$

Given that photo-Fenton requires that the Fe(III) species absorbs light and in order to increase the extinction coefficient of these Fe(III) salts while shifting the absorption wavelength towards the visible (Fe^{3+} aqueous solutions are slightly yellow), the photo-Fenton reaction is usually performed with organic complexes rather than aquated Fe(III). Iron(III) oxalate is frequently used for this purpose due its simplicity and due to the reluctance of oxalate to undergo photodegradation under photo-Fenton conditions, thus, allowing many turnovers before oxalate itself becomes degraded.

In a recent variant of this photo-Fenton process, Bössmann and Braun have reported the preparation of iron(II) trisbipydiryl inside the cavities of faujasite Y.[144] The preparation of this iron complex is an obvious extension of their work on encapsulated $Ru(bpy)_3^{2+}$, with or without having TiO_2 co-doping, commented on earlier in two previous sections. According to the authors, the success of the ship-in-a-bottle synthesis of $Fe(bpy)_3^{2+}$ relies to a large extent on the use of ethylene glycol as solvent to effect the homogeneous incorporation of the ligand. Subsequently, TiO_2 clusters are formed in the cavities of $Fe(bpy)_3^{2+}$@Y by oligomerisation of $TiCl_3$ gas. One problem related to the use of hazardous and explosive $TiCl_3$ is that oxygen has to be rigorously excluded during the formation of TiO_2. It can, however, be assumed that other TiO_2 precursors such as $Ti(O\text{–}i\text{Pr})_4$, $Ti{=}O^{2+}$ or $TiCl_4$ will work equally well in the preparation of these systems, provided that the oligomerisation is carried out under the appropriate conditions. The assembly of this and related multi-component photocatalytic systems by making use of the compartmentalized space provided by the zeolite pore system is an example of the potential of zeolites to hold in place photosensitizer, relays, active sites and other components in an organized way, thus, permitting the mimicking of the photosynthetic centres of algae and green leaves.

By using 2,4-xylidine as model pollutant for aromatic amines, it has been determined that the TiO_2-codoped $[Fe(bpy)_3^{2+}]$@Y system is an efficient photocatalyst for the enhanced photo-Fenton reaction in the presence of hydrogen peroxide as hydroxyl radical source.[144]

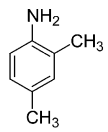

2,4-xylidine

It is expected that following this lead further developments of the photo-Fenton process will be reported using zeolite-based photocatalysts. Given that iron is a cheap reagent, the major contribution of heterogeneous photocatalysts based on inclusion in zeolite will be to increase light absorption of iron or iron complexes and the design of a continuous flow process avoiding the need of tedious flocculation of iron oxides.

Ion-exchanged zeolites as photocatalysts

The use of ion-exchanged zeolites is promising for the development of photocatalysts that decompose environmental pollutants. Some of these zeolites such as CuZSM-5 are also useful as non-photochemical catalysts for car exhaust gas treatment and other thermal de-NO_x, de-SO_x processes. Thus, not surprisingly Cu- and Ag-ion exchanged zeolites have been also studied as photocatalysts.[145] Using a combination of XAFS, photoluminescence

and diffuse reflectance optical measurements the coordination and aggregation state of these ions have been addressed.[145] These noble metal ions have been proposed to be monomers, dimers and clusters, their relative concentration strongly dependent on the zeolite host. Within ZSM-5, mordenite and Beta, these ions exist predominantly as isolated species with low coordination number[145] and they can act as photocatalysts for the decomposition of NO_x.[146] Simple ion exchange of ZSM-5 with Cu^{2+} followed by evacuation at temperatures higher than 100 °C is sufficient to transform Cu^{2+}-ZSM-5 into Cu^{+}-ZSM-5, according to EPR spectroscopy.[147,148] Interestingly, while Cu^{2+}-ZSM-5 does not emit, Cu^{+}-ZSM-5 exhibits an emission between 420–550 nm. Photoluminescence of Cu^{+}-ZSM-5 is quenched by NO proving the interaction of Cu^{+} excited state with NO. Cu^{+}-ZSM-5 photocatalytically decomposes NO into N_2 and O_2 at temperatures as low as 2 °C.[147,148]

Ag-containing zeolites have been tested for the removal of NO_x from air.[149–151] Ag(I)-ZSM-5 has been prepared and characterized spectroscopically in relation to its efficient photocatalytic activity for the decomposition of NO to N_2 and O_2. By combining measurements of photoluminescence and EXAFS with theoretical models the occurrence of several local environments for Ag^{+} ions and even the presence of $(Ag^{+})_n$ sites has been proposed. Calculations indicate that for NO coordinated to silver clusters, the N–O bond is stronger in the ground state, while for certain excited states the N–N and O–O bonds are stronger.[152]

Ag(I) ions exchanged within zeolite tend to become reduced either spontaneously or chemically forming clusters of silver metal encapsulated within the zeolite internal micropores. Calzaferri and co-workers have made significant contributions in the use of Ag@zeolite as photocatalysts. Depending on the aggregation state of these clusters and their size, the colour of the zeolite varies from white, yellow to red.[153] These zeolite-encapsulated silver clusters exhibit intense photoluminescence, with variable λ_{em} depending on the nuclearity of the silver clusters. Moreover, it has been found that intrazeolite energy transfer from monomer Ag sites (higher excited state energy) to oligomeric clusters (lower energy) is very efficient.

In an early report, Jacobs and co-workers studied the efficiency of zeolite-encapsulated Ag clusters for the photocatalytic splitting of water.[154] Similarly, Calzaferri reported that when silver zeolite A (Si/Al 1, pore size 3–5 Å) is illuminated in the presence of water molecular oxygen is evolved and Ag^{+} becomes reduced.[153] In the photochemical splitting of water, oxygen generation is always much more difficult than the photogeneration of H_2 since the process for oxygen formation requires four electrons and the mechanism goes through the intermediacy of a series of activated oxygen intermediates. The quantum yield of Ag@A for oxygen formation is high, reaching the maximum at neutral pH. An investigation of the spectral response shows an interesting effect known as *self-sensitisation*.[153] This term refers to the fact that while the initial photoresponse is only for UV wavelengths, the response extends gradually to the red reaching 600 nm as the reaction proceeds. The reason for this is that during the photochemical reaction, partially reduced Ag clusters are formed and these new chromophores shift the absorption band towards the red. The zeolite structure acts controlling the size of the clusters and, as a consequence of the operation of a quantum size regime, also controls the energy levels of the orbitals of the Ag clusters.[153] The major problem to solve to convert oxygen evolution in a truly photocatalytic process is the reoxidation of reduced Ag back to the original Ag(I) state.

On the other hand, it has also been reported that silver clusters entrapped on zeolite A can effect the photocatalytic decomposition of carbaryl, carbofuran and malathion with an efficiency that is 164, 120, and 35 times faster than the corresponding direct irradiation of the pesticides in the absence of any photocatalyst.[155] The efficiency of the photocatalytic degradation depends on the size of the Ag clusters, yellow and red Ag@A solids being less efficient.[155]

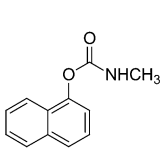

carbaryl

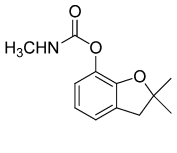

carbofuran

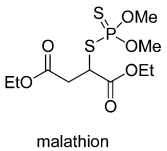

malathion

Rare-earth exchanged zeolites act as photocatalysts for the decomposition of N_2O into N_2 and O_2.[156] Praseodymium exchanged on mordenite or supported on alumina or silica-alumina has been found among the most efficient photocatalysts for this purpose.[156] Yoshida and co-workers have demonstrated[157] that Pr is present as isolated ions in the zeolite channels and that it is coordinated to four oxygen atoms and one Al atom. Other inactive Pr species surrounded by ten oxygen atoms including co-adsorbed water have also been characterized. Apparently, the low coordination of Pr atoms is necessary in order to bind with N_2O, supposedly the first step in the photocatalytic degradation.

Although considerably less explored than the photocatalysis aimed at pollutant remediation (*negative photocatalysis*), there are also some examples of *positive* photocatalysis. The latter type of photocatalysis tries to accomplish the synthesis of organic compounds using light and a photocatalyst. Perhaps the positive photocatalysis that has attracted the most attention is the red-light photooxidation of alkanes, alkenes and alkylaromatics by selective excitation of the contact charge transfer complexes between the hydrocarbons and oxygen within the cavities of alkali exchanged zeolites.[158–164] This subject has been recently covered in depth in several reviews.[165–167]

In solution it is known that alkenes and aromatic hydrocarbons form collisional charge-transfer complexes with molecular oxygen that can be characterized by the adsorption band. In zeolites, the same complex is also formed but it undergoes a dramatic stabilization, reflected by large shifts in the λ_{max} of the charge-transfer band that moves from the UV in organic solvents to the visible for the zeolite encapsulated collisional complex. In these photooxygenations, the zeolite plays a passive role defining a highly polar reaction cavity in which the actual photoactive charge-transfer complex becomes stabilized. By studying the influence of the alkali and alkali-earth charge-compensating cations on the red shift of the adsorption band, it has been demonstrated that the remarkable stabilization is due to the electrostatic fields experienced inside the zeolite cavities. Selective excitations of these charge-transfer hydrocarbon-oxygen complexes produces an electron transfer, followed by hydrogen abstraction yielding as photoproduct the corresponding hydroperoxide with almost complete selectivity. Besides simple alkenes and alkylaromatics, the photooxygenation through stabilized charge-transfer complexes also works for cyclohexane giving cycloalkyl hydroperoxide (Scheme 18).[163] This process could be interesting from the

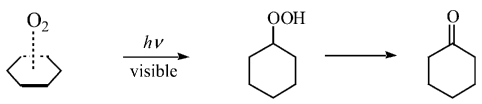

Scheme 18

industrial point of view in the context of ε-caprolactam production from cyclohexane and efforts to commercial this photocatalytic oxidation have been made.

Another example of positive photocatalysis is the formation of trans-1,4,6,9-tetraazabicyclo[4.4.0]decane by one step reaction of ethanol and ethylenediamine over TiO_2/zeolite photocatalyst with solar or artificial light at ambient temperature.[168] Among the zeolites that have been tested are HY, Hbeta and HZSM-5.

Polyoxometalates have a noticeable activity in the photoinduced oxidation of organic compounds including hydrocarbons.[169–179] The tetrabutylammonium salt of decatungstate $W_{10}O_{32}^{4-}$ has been

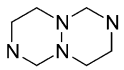

1,4,6,9-tetraazabicyclo[4.4.0]decane

supported on MCM-41 at loadings between 10 and 60 wt% and amorphous silica by simple impregnation.[179] Surface area and pore volume measurements indicates that $(n\text{-}Bu_4N)_4W_{10}O_{32}$ fills first the largest pores before filling the 30 Å channels of MCM-41, showing then a decrease in the total surface area and in the pore volume. Comparison of the photocatalytic activity of dissolved or supported $(n\text{-}Bu_4N)_4W_{10}O_{32}$ for the oxidation of dichloromethane solutions of cyclohexane and cyclododecane indicates that, in general, heterogeneization does not significantly decrease the photocatalytic efficiency of the polyoxometalate and can actually increase it as for the case of cyclododecane photooxygenation.[170] The photocatalysts can be reused at least three times without any loss in activity.

The products of the photocatalytic oxidation with decatungstate supported on silicas and MCM-41 are the corresponding cyclic alcohols and ketones in different one/ol ratios. The nature of the support exerts some control on the one/ol ratio that is thought to arise from differences in the adsorption coefficient of the reaction products on different supports.[170]

As consequence of the larger surface area of MCM-41 as compared to silica, MCM-41 is able to disperse up to a 30% in weight of $(n\text{-}Bu_4N)_4W_{10}O_{32}$ without a decrease in turnover number that normally accompanies polyoxometalate agglomeration. However, decatungstate supported on silica was found two-fold more active than the same polyoxometalate supported on MCM-41 or in solution for the photocatalytic oxidation of cyclododecane, something that has not been sufficiently explained and unsatisfactorily attributed to "*surface effects*". There is an optimum of supported decatungstate photocatalyst per ml of solvent. Initially there is an increase in the yield of oxidation products at a certain reaction time with the weight of dispersed photocatalyst up to a limit that corresponds to the maximum amount of illuminated photocatalyst. Then, for higher amounts of photocatalyst, no further increase in the initial activity is observed, since the number of photons captured by the photocatalyst does not increase but actually decreases by scattering and reflection.

Zeolites having photocatalytically active framework

Given that aluminosilicate zeolites do not exhibit any absorption in the UV or visible region, they are photochemically inactive. The first law of photochemistry requires that light absorption has to be the first event before any photochemical process occurs.[51,52] However, the presence of framework heteroatoms other than Si and Al may introduce some absorption band in the UV region, hence giving the opportunity for photochemical reactions to occur upon UV excitation. One example of the influence of the heteroatom on the photocatalytic activity is the introduction of Ti atoms in the zeolite framework. The most remarkable example of titanium-containing zeolites is titanosilicalite TS-1, a titanosilicate having MFI structure isostructural to silicalite or ZSM-5. TS-1 was first synthesized by ENI researchers and used as a selective catalyst for alkene epoxidation and aromatic hydroxylation among other reactions.[180–182] In this case, the presence of tetrahedral Ti atoms in framework positions is responsible for a characteristic absorption band at 225 nm, corresponding to the ligand-to-metal (–O–Ti≡) electron transfer occurring at isolated Ti atoms. It has been found that TS-1 (Si/Ti ratios from 3.3 to 26.3) can effect the photocatalytic decomposition of 4-nitrophenol from aqueous solutions.[183] The photocatalytic efficiency of TS-1 is largely influenced by the presence or absence of H_2O_2. In the absence of H_2O_2, the TS-1 sample having lower Si/Ti ratios and consequently large amounts of extraframework TiO_2 nanoparticles exhibited higher photocatalytic activity. In contrast, when the irradiation is carried out in the presence of H_2O_2 a remarkable enhancement of the photocatalytic activity is observed, with the TS-1 with the highest Si/Ti ratio the most active material. These results suggest that in the presence of H_2O_2, the photochemical irradiation generates ·OH radicals from the titanium-hydroperoxide complex formed by the interaction of framework titanium atoms in TS-1 with H_2O_2 (Scheme 19). It is known that only tetrahedral Ti atoms tripodally

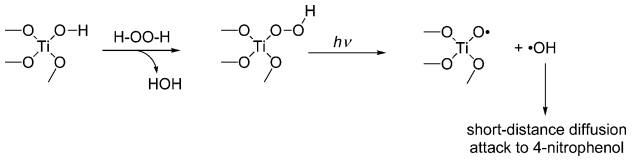

Scheme 19

connected to the TS-1 framework are able to form this titanohydroperoxy species. In addition, the capacity of TS-1 to adsorb 4-nitrophenol from aqueous solutions increases along with the Si/Ti ratio, and this factor also co-operates in the photocatalytic activity by bringing reactants and ·OH radicals in close proximity.[183]

Careful IR spectroscopic work by Lin and Frei has, however, led to an alternative proposal for the cleavage of the titanohydroperoxy group. These authors have shown that Ti silicalite upon addition of hydrogen peroxide and subsequent evacuation forms a hydroperoxy ≡Ti–OOH species characterized by a O–O stretch vibration at 837 cm^{-1}, shifting to 793 cm^{-1} for the ^{18}O-labelled species.[184] This ≡Ti–OOH species is indefinitely stable at room temperature and thermally stable up to 60 °C and exhibits a ligand-to-metal charge transfer band at λ_{max} 360 nm tailing up to 550 nm. It is supposed that this ≡Ti–OOH processes a η^2 configuration in where the oxygen of the OH group interacts with the Ti atom. When irradiated at the ligand-to-metal charge-transfer band, ≡Ti–OOH decomposes with an estimated quantum yield efficiency of unity to form a titanol group and an oxygen atom. Photolysis of the ≡Ti–OOH can oxidize ethylene to ethylene oxide or can accelerate the epoxidation of propylene.[184]

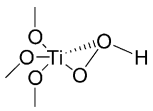

η^2 hydroperoxy species

Analogously, Ban *et al.* have studied the photocatalytic degradation of monoethanolamine using TS-1.[185] Framework Ti atoms form a complex with ethanolamine in aqueous solution as is evidenced by the observation by a characteristic absorption band at λ_{max} ~300 nm, compared to the initial absorption band of TS-1 appearing at λ ~ 220 nm. Photoexcitation of the ethanolamine-framework Ti complex leads to the degradation of the organic amine. TiO_2 is also able to effect the photocatalytic degradation of ethanolamine, giving rise to a similar product distribution as that observed for TS-1. The photocatalytic activity per weight of photocatalyst was lower for TS-1 than TiO_2, but the intrinsic activity per Ti atom in TS-1 is higher than that in TiO_2, something that reflects the benefits of site isolation in TS-1 and the sieving properties of this porous zeolite.

Corma et al. were the first to prepare (Ti)Beta zeolite and use this zeolite for the selective oxidation of alkenes in the presence of organic hydroperoxides.[186] Anpo has shown that (Ti)Beta zeolites can effect the photocatalytic reduction of CO_2 with H_2O at 50 °C to CH_4 and CH_3OH. Combining the information of XAFS, absorption spectroscopy and photoluminescence it was demonstrated that isolated tetrahedral Ti atoms are responsible for this photoactivity. Furthermore, the hydrophilic or hydrophobic nature of the (Ti)Beta photocatalyst strongly influences the interaction of Ti atoms with water.[77]

Highly dispersed titanium oxide within the mesoporous FSM-16 silicate can be prepared by a chemical vapour deposition method. The resulting solid acts as an efficient photocatalyst for the reduction of CO_2 with H_2O at 55 °C to produce methane and methanol, with high selectivity towards the latter. It has been found that a good correlation exist between the activity of the photocatalyst and its photoluminescence yield, leading to the suggestion that the group responsible for the two phenomena coincide. This is taken as evidence that isolated, tetrapodal, framework ≡Ti–O– is the photochemically active group.[76]

The optical properties of nanocrystalline anatase powders or thin films depend on the drying and sintering procedure and not exclusively on the primary particle size. It has been proposed that the electronic properties of these TiO_2 nanoparticles are determined by surface phenomena rather than quantum size effects. In this regard, it has been argued that novel titanosilicate ETS-10 which contains monodimensional quantum wires of TiO_2 embedded into an isolating siliceous matrix could be a suitable system for studying quantum size effects on TiO_2.[187] The photoactivity of titanosilicalite ETS-10 arises from the presence of photoexcitable Ti–O–Ti chains while the tridirectional 12 membered channel system (0.8 × 0.5 nm) endows the material with excellent adsorption capacity characteristic of zeolites.[188,189] Zecchina, Pelizzetti and co-workers have shown that ETS-10 can act as a shape-selective photocatalyst for the degradation of a mixture of phenols of different sizes.[190] Those compounds small enough to access the interior of the micropores become protected and are degraded more slowly, while those others that are too large to enter the pores are degraded preferentially. These results have been interpreted in terms of the protective role played by the internal pore system of ETS-10, degradation of the organic molecules occurring mainly at the external surface. In agreement with this hypothesis, mild post-synthesis treatment of ETS-10 with diluted hydrofluoric acid increases the photocatalytic activity of ETS-10 by dissolving preferentially SiO_4 without causing a drastic damage of the solid structure, and preserving the shape-selectivity of the photodegradation.[191] In this way the photoactivity of treated ETS-10 is comparable or even better than that of unselective TiO_2.

Like titanosilicates, other transition metals such as V and Cr have been incorporated inside the silicalite framework and the resulting solids tested for the photocatalytic degradation of NO_x.[192] Framework incorporation is believed to increase the intrinsic activity of the photocatalytic transition metal but shifts the excitation radiation to shorter wavelengths as compared to their corresponding bulk oxides. This effect is generally undesirable since irradiation requires UV lamps and quartz glassware and an optimum photocatalyst should be able to operate with ambient visible light through glass. To overcome this negative blue-shift effect of framework incorporation, Anpo and co-workers have suggested ion doping that can expand the absorption band of framework Ti to the visible region.[192]

Vanadium silicalite VS-2 has been obtained by hydrothermal synthesis and the resulting solid characterized by XANES, EXAFS, ESR, FT-IR, UV-Vis, solid state NMR and XRD techniques.[150] The data are compatible with the presence of tetrahedral V species having a terminal V=O group, tripodally grafted to the framework. UV irradiation of VS-2 is able to effect the photocatalytic decomposition of NO to N_2, O_2 and NO_2.[150] It has been proposed that the mechanism involves charge transfer from the excited state of ≡V=O to NO.

Most of the reports on the photocatalytic activity of zeolites and related porous silicates focus on materials containing framework heteroatoms others than Si or Al. Furthermore, it is a general belief that silica materials are (photo)catalytically inert. However, this widely-accepted assumption is not completely true in view that porous silica acts as photocatalysts.[193–204] Yoshida and co-workers have demonstrated that mesoporous *all-silica* MCM-41 and FSM-16 act as photocatalysts for the metathesis of propene (eqn. (3)) upon irradiation with low pressure Hg lamp (most intense irradiation wavelength at 254 nm).

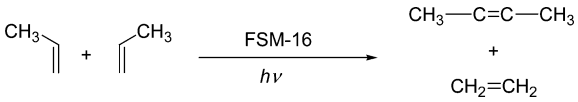

(3)

Pre-treatment of the all-silica mesoporous silicate at temperatures above 400 °C is essential for the appearance of the photocatalytic activity. This has lead to the conclusion that the photocatalytic sites are strained siloxane bridges formed through dehydroxylation of isolated silanol groups (eqn. (4)). Spectroscopic evidence in support of these strained siloxane bridges are the disappearance in the IR of the band corresponding to isolated silanols at 3745 cm^{-1} and the appearance of new absorption bands at 910 and 891 cm^{-1}. The activity of the silicate photocatalysts studied follows the order FSM-16 > MCM-41 > amorphous silica. The presence of Al in the composition of the mesoporous silicate does not increase the efficiency of the photocatalytic propene metathesis, indicating that this element does not play any role in the process and NH_3 treatment completely deactivates the silicate. In view of this, it would be of interest to expand these results to other materials that contain a large density of silanol groups such as ITQ-2.

(4)

Concerning the mechanism of the photometathesis in the first stages the real active site is formed on the silica surface by photoreaction of the strained siloxane group and propene, before a chain mechanism is initiated (eqn. (5))

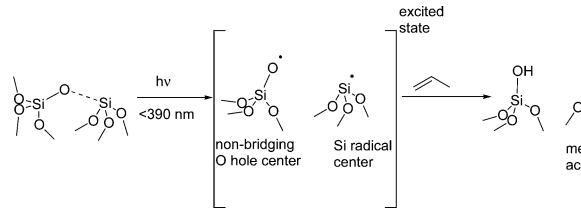

(5)

Prospects and concluding remarks

This account has illustrated the potential of zeolite-based photocatalysts for the degradation of pollutants and malodorous compounds in air and water. Given the current concern in environmental issues, it can be foreseen that application of these systems will be growing at increasing speed, particularly for gas and air treatments. For gas phase photodegradations, the transparency of the medium and the ease to develop continuous flow photoreactors has already allowed commercialisation of photocatalysts pollutant degradation using small domestic devices. Daikin has already sold over 1 000 000 units of air purifiers based on photocatalysis in Japan, the European market being more reluctant to the growth. Far from immediate application, and where big improvement of the photocatalysis is still needed, are potentially large-scale industrial processes such as de-NO_x and CO_2 fixation.

In the case of waste waters, deactivation and reactivation are more demanding issues that require a detailed study in each case. For waste water, the opacity of the medium may make necessary a pre-treatment to increase transparency. In addition to the cost of the photocatalyst, another factor that limits application of photocatalysis in general is the relative high cost of electrical energy. Solar irradiation and more efficient photoreactors are needed to overcome the comparatively high price of photocatalysis. Photo-

catalytic disinfection, to potabilise water in small local facilities seems to be viable using solar light.

Finally, it can be foreseen that related with the renewed interest in the photocatalytic splitting of water, new technologies will emerge in the near future that will try to develop positive photocatalysis for the generation of hydrogen and oxygen as well as for the synthesis of chemicals. Here, most of the processes are still studied from the fundamental point of view and at laboratory scale.

It can also be anticipated that further and more elaborated multicomponent systems will be developed in which the zeolite internal voids will be used to build spatially organized, multifunctional photocatalysts.

Acknowledgements

Financial support of the Spanish Ministry of Science and Technology (MAT 2003-1226 and MAT2003-07945-C02-01) and Generalidad Valenciana (grupos 03-020) is gratefully acknowledged.

Notes and references

1 R. M. Barrer, *Zeolites and Clay Minerals as Sorbents and Molecular Sieves*, Academic Press, London, 1978.
2 D. W. Breck, *Zeolite Molecular Sieves: Structure, Chemistry and Use*, John Wiley and Sons, New York, 1974.
3 *Introduction to Zeolite Science and Practice*, ed. H. van Bekkum, E. M. Flanigen and J. C. Jansen, Elsevier, Amsterdam, 1991.
4 W. M. Meier, D. H. Olson and C. Baerlocher, *Zeolites*, 1996, **17**, 1–229.
5 M. E. Davis, *Acc. Chem. Res.*, 1993, **26**, 111–115.
6 M. E. Davis, *Chem. Eur. J.*, 1997, **3**, 1745–1750.
7 *Photochemistry in Organized and Constrained Media*, ed. V. Ramamurthy, VCH, New York, 1991.
8 H.-R. Tseng, S. A. Vignon, P. C. Celestre, J. F. Stoddart, A. J. P. White and D. J. Williams, *Chem. Eur. J.*, 2003, **9**, 543–556.
9 F. M. Raymo and J. F. Stoddart, *Polym. Mater. Sci. Eng.*, 1999, **80**, 33–34.
10 C. Hamers, O. Kocian, F. M. Raymo and J. F. Stoddart, *Adv. Mater.*, 1998, **10**, 1366–1369.
11 V. Balzani, A. Credi, F. M. Raymo and J. F. Stoddart, *Angew. Chem. Int. Ed.*, 2000, **39**, 3348–3391.
12 A. Starosud, A. Bhargava, C. H. Langford and A. Kantzas, *Stud. Surf. Sci. Catal.*, 1999, **122**, 219–228.
13 F. Marquez, H. Garcia, E. Palomares, L. Fernandez and A. Corma, *J. Am. Chem. Soc.*, 2000, **122**, 6520–6521.
14 F. Marquez, C. M. Zicovich-Wilson, A. Corma, E. Palomares and H. Garcia, *J. Phys. Chem. B*, 2001, **105**, 9973–9979.
15 F. Marquez, V. Marti, E. Palomares, H. Garcia and W. Adam, *J. Am. Chem. Soc.*, 2002, **124**, 7264–7265.
16 A. R. Pradhan, M. A. Macnaughtan and D. Raftery, *J. Am. Chem. Soc.*, 2000, **122**, 404–405.
17 H. Garcia and H. D. Roth, *Chem. Rev.*, 2002, **102**, 3947–4008.
18 N. Herron, G. D. Stucky and C. A. Tolman, *J. Chem. Soc., Chem. Commun.*, 1986, 1521.
19 N. Herron, *Inorg. Chem.*, 1986, **25**, 4714–17.
20 D. Wohrle, A. K. Sobbi, O. Franke and G. Schulz-Ekloff, *Zeolites*, 1995, **15**, 540–550.
21 N. Herron, *J. Coord. Chem.*, 1988, **19**, 25–38.
22 G. Schulz-Ekloff and S. Ernst, *Prep. Solid Catal.*, 1999, 405–427.
23 R. A. Sheldon, I. W. C. E. Arends and H. E. B. Lempers, *Catal. Today*, 1998, **41**, 387–407.
24 J. Weitkamp, U. Weiss and S. Ernst, *Stud. Surf. Sci. Catal.*, 1995, **94**, 363–80.
25 K. J. Balkus, Jr., A. K. Khanmamedova, K. M. Dixon and F. Bedioui, *Appl. Catal., A*, 1996, **143**, 159–173.
26 A. Corma and H. Garcia, *Top. Catal.*, 1998, **6**, 127–140.
27 A. Corma and H. García, *J. Chem. Soc., Dalton Trans.*, 2000, 1381–1394.
28 W. De Wilde, G. Peeters and J. H. Lunsford, *J. Phys. Chem.*, 1980, **84**, 2306–2310.
29 P. K. Dutta and M. Puri, *J. Catal.*, 1988, **111**, 453–456.
30 P. K. Dutta, W. Turbeville and D. S. Robins, *J. Phys. Chem.*, 1992, **96**, 5024–5029.
31 P. K. Dutta, *J. Incl. Phen. Molec. Recognition. Chem.*, 1995, **21**, 215–237.
32 M. Alvaro, G. A. Facey, H. García, S. García and J. C. Scaiano, *J. Phys. Chem.*, 1996, **100**, 18173–18176.
33 A. Corma, V. Fornes, M. S. Galletero, H. Garcia and J. C. Scaiano, *Chem. Commun.*, 2002, 334–335.
34 Y. S. Park, E. J. Lee, Y. S. Chun, Y. D. Yoon and K. B. Yoon, *J. Am. Chem. Soc.*, 2002, **124**, 7123–7135.
35 M. Sykora, K. Maruszewski, Z. Treffet, M. Shelly and J. R. Kincaid, *J. Am. Chem. Soc.*, 1998, **120**, 3490.
36 J. R. Kincaid, *Chem. Eur. J.*, 2000, **6**, 4055–4061.
37 M. Sykora and J. R. Kincaid, *Nature*, 1997, **387**, 162–164.
38 A. K. Aboul-Gheit and S. M. Ahmed, *Stud. Surf. Sci. Catal.*, 2001, **135**, 5011–5019.
39 W. Adam, A. Corma, H. Garcia and O. Weichold, *J. Catal.*, 2000, **196**, 339–344.
40 K. J. Balkus, Jr., *Phthalocyanines*, 1996, **4**, 285–305.
41 M. A. Miranda and H. García, *Chem. Rev.*, 1994, **94**, 1063.
42 A. Corma, V. Fornés, H. García, M. A. Miranda, J. Primo and M. J. Sabater, *J. Am. Chem. Soc.*, 1994, **116**, 2276.
43 The symbol ″@″ has been introduced by N. J. Turro to indicate a guest incorporated inside a host.
44 A. M. Amat, A. Arques, S. H. Bossmann, A. M. Braun, S. Gob and M. A. Miranda, *Angew. Chem. Int. Ed.*, 2003, **42**, 1653–1655.
45 A. Corma, V. Fornés, H. García, M. A. Miranda and M. J. Sabater, *J. Am. Chem. Soc.*, 1994, **116**, 9767–9768.
46 A. Sanjuan, M. Alvaro, A. Corma and H. Garcia, *Chem. Commun.*, 1999, 1641–1642.
47 A. Corma and H. García, *Chem. Rev.*, 2002, **102**, 3837–3892.
48 A. Sanjuan, G. Aguirre, M. Alvaro and H. Garcia, *Appl. Catal., B*, 1998, **15**, 247–257.
49 A. Sanjuan, G. Aguirre, M. Alvaro, H. Garcia and J. C. Scaiano, *Appl. Catal., B*, 2000, **25**, 257–265.
50 M. Alvaro, E. Carbonell, H. García, C. Lamaza and M. N. Pillai, *Photochem. Photobiol. Sci.*, 2004, **3**((9)), 189–89.
51 N. J. Turro, *Modern Molecular Photochemistry*, Benjamin Cummings, Menlo Park, 1978.
52 A. Gilbert and J. Baggott, *Essentials of Organic Photochemisry*, Blackwell, Oxford, 1990.
53 M. V. Baldoví, F. L. Cozens, V. Fornés, H. García and J. C. Scaiano, *Chem. Mater.*, 1996, **8**, 152–160.
54 M. A. Miranda, H. García and M. L. Cano, in *Vergleich der photosensibilisierten Dimerisierung von 1,3–Cyclohexadien. Elektronen– versus Energietransfer Mechanismus*, ed. D. Wöhrle, M. W. Tausch, and W. D. Stohrer, Verlag Chemie, Weinheim, 1998.
55 F. Müller and J. Mattay, *Chem. Rev.*, 1993, **93**, 99–117.
56 T. Yashima, J. H. Kim, H. Ohta, S. Namba and T. Komatsu, *Stud. Surf. Sci. Catal.*, 1994, **90**, 379–389.
57 C. B. Khouw and M. E. Davis, *ACS Symp. Ser.*, 1993, **517**, 206–221.
58 N. Y. Chen, W. E. Garwood and F. G. Dwyer, *Shape Selective Catalysis in Industrial Applications*, Marcel Dekker, New York, 1989.
59 M. V. Baldoví, A. Corma, H. García and V. Martí, *Tetrahedron Lett.*, 1994, **35**, 9447–9450.
60 V. Ramamurthy, P. Lakshminarasimhan, P. C. Grey and L. Johnston, *Chem. Commun.*, 1998, 2411.
61 M. Kasha and D. E. Brabham, in *Singlet oxygen electronic structure and photosensitization*, ed. H. H. Wasserman and R. W. Murray, New York, 1979.
62 E. L. Clennan, *Tetrahedron*, 2000, **56**, 9151–9179.
63 E. L. Clennan, in *Molecular Oxygenations in Zeolites*, ed. V. Ramamurthy and Schanze, New York, 2002.
64 E. L. Clennan and J. P. Sram, *Tetrahedron Lett.*, 1999, **40**, 5275–5278.
65 M. Stratakis and G. Froudakis, *Org. Lett.*, 2000, **2**, 1369–1372.
66 M. Stratakis and G. Kosmas, *Tetrahedron Lett.*, 2001, **42**, 6007–6009.
67 M. Stratakis and C. Rabalakos, *Tetrahedron Lett.*, 2001, **42**, 4545–4547.
68 X. Li and V. Ramamurthy, *J. Am. Chem. Soc.*, 1996, **118**, 10666–10667.
69 S. Zhang, T. Kobayashi, Y. Nosaka and N. Fujii, *Denki Kagaku oyobi Kogyo Butsuri Kagaku*, 1995, **63**, 927–31cf. CA 1995:858448.
70 X. Liu, K. K. Iu and J. K. Thomas, *J. Chem. Soc., Faraday Trans.*, 1993, **89**, 1861–5.
71 S.-E. Park, J.-S. Hwang, J.-S. Chang, J.-M. Kim, D. S. Kim and H. S. Chai, US, 2002, 2002098977.

72 S. Corrent, G. Cosa, J. C. Scaiano, M. S. Galletero, M. Alvaro and H. García, *Chem. Mater.*, 2001, **13**, 715–722.
73 M. Anpo, *Catal. Surv. Jap.*, 1997, **1**, 169–179.
74 G. Cosa, M. S. Galletero, L. Fernández, F. Márquez, H. García and J. C. Scaiano, *New J. Chem.*, 2002, **26**, 1448–1455.
75 K. Ikeue, H. Yamashita and M. Anpo, *Electrochemistry*, 2002, **70**, 402–408.
76 K. Ikeue, H. Yamashita and M. Anpo, *Chem. Lett.*, 1999, 1135–1136.
77 K. Ikeue, H. Yamashita, M. Anpo and T. Takewaki, *J. Phys. Chem. B*, 2001, **105**, 8350–8355.
78 Y. Kim and M. Yoon, *J. Mol. Catal. A*, 2001, **168**, 257–263.
79 K. Takaya, Jp, 2000, 2000084544.
80 T. Domoto, Jp, 1998, 10230134.
81 N. Egashira, Jp, 2000, 2000126279.
82 K. Kuchino and S. Tokumitsu, Jp, 2000, 2000117118.
83 H. Yoneyama and T. Torimoto, *Catal. Today*, 2000, **58**, 133–140.
84 T. Shimizu, Y. Fujita, K. Yanagihara, T. Takehana and K. Murakami, Jp, 2000, 2000107270.
85 K. Nishikawa and N. Arai, Jp, 2000, 2000102597.
86 H. Nojima, A. Miyata, K. Suzuki and T. Watsuji, Jp, 2000, 2000084056.
87 T. Nakajima, Jp, 1999, 11290697.
88 Y. Kitamura, Y. Sakane and H. Yajima, Jp, 1999, 11253931.
89 K. Nishikawa, Jp, 1999, 11137656.
90 S. Koura and K. Sakato, Jp, 1998, 10314599.
91 C. Morishige, M. Sato, S. Kobase and Y. Takekawa, Jp, 1998, 10296920.
92 K. Yoshioka, N. Fukazawa, I. Ono, H. Fujii, T. Okuda and Y. Uemoto, Jp, 1998, 10263413.
93 Y. Sakane, Jp, 1998, 10127741.
94 T. Ariga, Jp, 1998, 10094587.
95 K. Takimoto, Jp, 1997, 09161537.
96 T. So, M. Sato, H. Kawahara and S. Ohara, Jp, 1997, 09206200.
97 T. Mune and M. Sato, *Kino Zairyo*, 1996, **16**, 12–21*cf.* CA 1996:542601.
98 O. Tahara and K. Omatsu, Jp, 2000, 2000107609.
99 T. Usami, Jp, 1999, 11319570.
100 K. Nishikawa, Jp, 2000, 2000210372.
101 T. Usami, K. Mochizuki, M. Utsumi, K. Kinoshita, T. Iwata and K. Kagawa, Jp, 2000, 2000051333.
102 T. Arika and H. Yajima, Jp, 1998, 10249209.
103 S. Koura, A. Ando and K. Sakato, Jp, 2000, 2000042366.
104 S. Koura, A. Ando and K. Sakato, Jp, 2000, 2000061310.
105 A. Fujishima, K. Hashimoto, M. Takada, S. Kamiyama and K. Matsubara, Jp, 1997, 09206602.
106 S. Murasawa, H. Murakami, Y. Fukui, M. Watanabe, A. Fujishima and K. M. Hashimoto, Ep, 1995, 633064.
107 T. Sakuramoto, M. Urairi, M. Sugimoto and T. Domoto, Jp, 1997, 09278928.
108 N. Takeda, M. Ohtani, T. Torimoto, S. Kuwabata and H. Yoneyama, *J. Phys. Chem. B*, 1997, **101**, 2644–2649.
109 T. Usami, Jp, 1999, 11155479.
110 M. Sakura, Jp, 1995, 07016473.
111 H. Nakamura and S. Koura, Jp, 2002, 2002115176.
112 K. Mori and M. Nakamura, Jp, 2001, 2001181535.
113 K. Yamagata, Jp, 1999, 11333451.
114 C. H. Langford and Y. Xu, Wo, 1996, 9626903.
115 M. Kitamura and J. Fujita, Jp, 1996, 08228636.
116 H. Honda, Y. Ito and K. Saito, Jp, 2000, 2000096430.
117 N. Ito, H. Honda and K. Saito, Jp, 2001, 2001254263.
118 K. Okamoto, S. Hishinuma and S. Tabuchi, Jp, 2001, 2001254275.
119 K. Okamoto, S. Hishinuma, M. Ishige, K. Adachi and H. Okamura, Jp, 2001, 2001254265.
120 M. Umeda , T. Jinbo and H. Honda, Jp, 2001, 2001254267.
121 K. Okada, Jp, 1996, 08319205.
122 O. Beaune, A. Finiels, P. Geneste, P. Graffin, A. Guida, J. L. Olive and A. Saeedan, *Stud. Surf. Sci. Catal.*, 1993, **78**, 401–408.
123 M. Anpo, H. Yamashita, M. Matsuoka, D.-R. Park, Y.-G. Shul and S.-E. Park, *J. Ind. Eng. Chem.*, 2000, **6**, 59–71.
124 Y. Ichihashi, S. Zhang, H. Yamashita and M. Anpo, *Hyomen*, 1996, **34**, 516–526, *cf.* CA 1996:622329.
125 J. Zhang, Y. Hu, M. Matsuoka, H. Yamashita, M. Minagawa, H. Hidaka and M. Anpo, *J. Phys. Chem. B*, 2001, **105**, 8395–8398.
126 X. Domenech and J. Peral, *Chem. Ind.*, 1989, 606.
127 A. I. Kryukov, A. V. Korzhak, G. M. Tel'biz, V. G. Il'in and S. Y. Kuchmii, *Theor. Exp. Chem.*, 1998, **34**, 93–98.
128 A. V. Korzhak, S. Y. Kuchmij, G. M. Telbiz, N. F. Guba, V. G. Ilin, A. I. Kryukov and V. D. Pokhodenko, Su, 1994, 1732621.
129 Y. I. Kim, S. W. Keller, J. S. Krueger, E. H. Yonemoto, G. B. Saupe and T. E. Mallouk, *J. Phys. Chem. B*, 1997, **101**, 2491.
130 J. S. Krueger, J. E. Mayer and T. E. Mallouk, *J. Am. Chem. Soc.*, 1988, **110**, 8232.
131 L. Persaud, A. J. Bard, A. Champion, M. A. Fox, T. E. Mallouk, S. E. Webber and J. M. White, *J. Am. Chem. Soc.*, 1987, **109**, 7309.
132 B. J. Aronson, C. F. Blanford and A. Stein, *Chem. Mater.*, 1997, **9**, 2842–2851.
133 S. H. Bossmann, C. Turro, C. Schnabel, M. R. Pokhrel, L. M. Payawan, Jr., B. Baumeister and M. Woerner, *J. Phys. Chem. B*, 2001, **105**, 5374–5382.
134 S. Bossmann, *GIT Labor-Fachzeitschrift*, 1997, **41**, 44–46.
135 G. Cosa, M. N. Chretien, M. S. Galletero, V. Fornes, H. Garcia and J. C. Scaiano, *J. Phys. Chem. B*, 2002, **106**, 2460–2467.
136 A. Hagfeldt and M. Gratzel, *Acc. Chem. Res.*, 2000, **33**, 269.
137 S. H. Bossmann, D. Herrmann, A. M. Braun and C. Turro, *J. Inf. Record.*, 1998, **24**, 271–275.
138 E. S. Brigham, P. T. Snowden, Y. I. Kim and T. E. Mallouk, *J. Phys. Chem.*, 1993, **97**, 8650.
139 L. Khouchaf, M. H. Tuilier, J. Durr, M. Wark and H. Kessler, *J. Phys. IV*, 1996, **6**, C4/939–C4/945.
140 G. Tel'biz, A. Shwets, V. Gun'ko, J. Stoch, G. Tamulajtis and N. Kukhtarev, *Stud. Surf. Sci. Catal.*, 1994, **84**, 1099–106.
141 D. F. Ollis and H. Al-Ekabi, in *Photocatalytic Purification and Treatment of Water and Air*, Amsterdam, 1993.
142 O. Legrini, E. Oliveros and A. M. Braun, *Chem. Rev.*, 1993, **93**, 671–698.
143 M. A. Malati, *Environ. Technol.*, 1995, **16**, 1093–1099.
144 S. H. Bossmann, N. Shahin, H. Le Thanh, A. Bonfill, M. Worner and A. M. Braun, *Chem. Phys. Chem.*, 2002, **3**, 401–407.
145 H. Yamashita, M. Matsuoka, M. Anpo and M. Che, *J. Phys. IV*, 1997, **7**, 941–942.
146 M. Matsuoka, H. Yamashita and M. Anpo, *Hyomen*, 1995, **33**, 773–81cf. CA 1996:132057.
147 M. Anpo, Y. Shioya, H. Yamashita, E. Giamello, C. Morterra, M. Che, H. H. Patterson, S. Webber and S. Ouellette, *J. Phys. Chem.*, 1994, **98**, 5744–50.
148 M. Anpo, T. Nomura, Y. Shioya, M. Che, D. Murphy and E. Giamello, *Stud. Surf. Sci. Catal.*, 1993, **75**, 2155–8.
149 K. Yoshida and Y. Yamashita, Jp, 1999, 11028365.
150 M. Anpo, S. G. Zhang, M. Matsuoka and H. Yamashita, *Catal. Today*, 1997, **39**, 159–168.
151 K. Mishima, S. Anho and H. Yamashita, Jp, 1996, 08099020.
152 S. M. Kanan, M. A. Omary, H. H. Patterson, M. Matsuoka and M. Anpo, *J. Phys. Chem. B*, 2000, **104**, 3507–3517.
153 G. Calzaferri, *Photochem. Photoelectrochem. Convers. Storage Sol. Energy, Proc. Int. Conf., 9th*, 1993, 141–57.
154 P. A. Jacobs, J. B. Uytterhoeven and H. K. Beyer, *J. Chem. Soc., Chem. Commun.*, 1977, 128–9.
155 H. H. Patterson, S. M. Kanan and M. C. Kanan, *Abstr. Pap. – Am. Chem. Soc.*, 2000, **220th**, INOR-179.
156 K. Ebitani, Y. Hirano and A. Morikawa, *J. Catal.*, 1995, **157**, 262–5.
157 K. Ebitani, A. Nishi, Y. Hirano, H. Yoshida, T. Tanaka, T. Mizugaki, K. Kaneda and A. Morikawa, *J. Synchrotron Radiat.*, 2001, **8**, 481–483.
158 F. Blatter and H. Frei, *J. Am. Chem. Soc.*, 1993, **115**, 7501–7502.
159 F. Blatter, F. Moreau and H. Frei, *J. Phys. Chem.*, 1994, **98**, 13403–13407.
160 F. Blatter and H. Frei, *J. Am. Chem. Soc.*, 1994, **116**, 1812–1820.
161 S. Vasenkov and H. Frei, *J. Phys. Chem. B*, 1998, **102**, 8177–8182.
162 S. Vasenkov and H. Frei, *J. Phys. Chem. B*, 1997, **101**, 4539–4543.
163 H. Sun, F. Blatter and H. Frei, *J. Am. Chem. Soc.*, 1996, **118**, 6873–6879.
164 H. Sun, F. Blatter and H. Frei, *J. Am. Chem. Soc.*, 1994, **116**, 7951–7952.
165 F. Blatter, H. Sun, S. Vasenkov and H. Frei, *Catal. Today*, 1998, **41**, 297–309.
166 H. Frei, F. Blatter and H. Sun, *Chemtech*, 1996, **26**, 24.
167 H. Sun, F. Blatter and H. Frei, in *Heterogeneous Hydrocarbon Oxidation*, ed. S. T. Oyama and B. K. Warren, Washington D.C., 1996.
168 K. V. S. Rao, B. Srinivas, A. R. Prasad and M. Subrahmanyam, *Chem. Lett.*, 2002, 236–237.

169 C. L. Hill and C. M. Prosser-McCartha, in *Photosensitization and Photocatalysis using Inorganic and Organometallic Compounds*, Dordrecht, 1993.
170 A. Maldotti, A. Molinari, G. Varani, M. Lenarda, L. Storaro, F. Bigi, R. Maggi, A. Mazzacani and G. Sartori, *J. Catal.*, 2002, **209**, 210–216.
171 R. Neumann and M. Dahan, *Nature*, 1997, **388**, 353.
172 C. L. Hill and C. M. Prosser-McCartha, *Coord. Chem. Rev.*, 1995, **143**, 407.
173 R. C. Chambers and C. L. Hill, *Inorg. Chem.*, 1989, **28**, 2509.
174 A. Hiskia and E. Papaconstantinou, *Inorg. Chem.*, 1992, **31**, 163.
175 L. P. Ermolenko and C. Giannotti, *J. Chem. Soc, Perkin Trans.*, 1996, 1205.
176 D. C. Duncan and C. L. Hill, *J. Am. Chem. Soc.*, 1997, **119**, 243.
177 C. Tanilean, K. Duffy and A. Jones, *J. Phys. Chem. B*, 1997, **101**, 4276.
178 A. Molinari, R. Amadelli, V. Carassiti and A. Maldotti, *Eur. J. Inorg. Chem.*, 2000, 91.
179 A. Molinari, R. Amadelli, L. Andreotti and A. Maldotti, *J. Chem. Soc., Dalton Trans.*, 1999, 1203.
180 G. Bellussi, A. Carati, M. G. Clerici, A. Esposito, R. Millini and F. Buonomo, Belgium, 1989, BE 1001038.
181 M. G. Clerici, *Appl. Catal.*, 1991, **68**, 249–61.
182 M. G. Clerici, *Fine chemicals through heterogeneous catalysis*, ed. R. A. Sheldon and H. Van Bekkum, Wiley-VCH, Weinheim, 2001.
183 G. D. Lee, S. K. Jung, Y. J. Jeong, J. H. Park, K. T. Lim, B. H. Ahn and S. S. Hong, *Appl. Catal., A*, 2003, **239**, 197–208.
184 W. Lin and H. Frei, *J. Am. Chem. Soc.*, 2002, **124**, 9292–9298.
185 T. Ban, S. Kondoh, Y. Ohya and Y. Takahashi, *Phys. Chem. Chem. Phys.*, 1999, **1**, 5745–5752.
186 A. Corma, M. A. Camblor, P. Esteve, A. Martínez and J. Pérez-Pariente, *J. Catal.*, 1994, **145**, 151–158.
187 T. Hanley, Y. Krisnandi, A. Eldewik, V. Luca and R. Howe, *Ionics*, 2001, **7**, 319–326.
188 R. F. Howe and Y. K. Krisnandi, *Chem. Commun.*, 2001, 1588–1589.
189 M. A. Fox, K. Doan and M. T. Dulay, *Res. Chem. Intermed.*, 1994, **20**, 711–722.
190 P. Calza, C. Pazè, E. Pelizzetti and A. Zecchina, *Chem. Commun.*, 2001, 2130–2131.
191 F. X. Llabrés i Xamena, P. Calza, C. Lamberti, C. Prestipino, A. Damin, S. Bordiga, E. Pelizzetti and A. Zecchina, *J. Am. Chem. Soc.*, 2003, **125**, 2264–2271.
192 M. Anpo, S. Higashimoto and M. Matsuoka, *Eco Ind.*, 1999, **4**, 11–19.
193 Y. Inaki, H. Yoshida, T. Yoshida and T. Hattori, *J. Phys. Chem. B*, 2002, **106**, 9098–9106.
194 M. Anpo, C. Yun and K. Kubokawa, *J. Catal.*, 1980, **61**, 267.
195 K. Kubokawa, M. Anpo and C. Yun, *Proc. 7th Int. Congress Catal.*, 1980, 171.
196 A. Ogata, A. Kazukawa and M. Enyo, *J. Phys. Chem.*, 1986, **90**, 5201.
197 H. Yoshida, T. Tanaka, M. Yamamoto, T. Funabiki and S. Yoshida, *Chem. Commun.*, 1996, 2125–2126.
198 H. Yoshida, T. Tanaka, M. Yamamoto, T. Yoshida, T. Funabiki and S. Yoshida, *J. Catal.*, 1997, **171**, 351.
199 H. Yoshida, T. Tanaka, S. Matsuo, T. Funabiki and S. Yoshida, *J. Chem. Soc., Chem. Commun.*, 1995, 761.
200 T. Tanaka, S. Matsuo, T. Maeda, H. Yoshida, T. Funabiki and S. Yoshida, *Appl. Surf. Sci.*, 1997, **121/122**, 296.
201 H. Yoshida, C. Murata, Y. Inaki and T. Hattori, *Chem. Lett.*, 1998, 1121.
202 H. Yoshida, K. Kimura, Y. Inaki and T. Hattori, *Chem. Commun.*, 1997, 129–130.
203 Y. Inaki, H. Yoshida and T. Hattori, *J. Phys. Chem. B*, 2000, **104**, 10304.
204 Y. Inaki, H. Yoshida, K. Kimura, S. Inagaki, Y. Fukushima and T. Hattori, *Phys. Chem. Chem. Phys.*, 2000, **2**, 5293.